

# Upregulated DNA Damage-Linked Biomarkers in Parkinson's Disease Model Mice

ASN Neuro  
Volume 15: 1–18  
© The Author(s) 2023  
Article reuse guidelines:  
sagepub.com/journals-permissions  
DOI: 10.1177/17590914231152099  
journals.sagepub.com/home/asn



Fei Zeng<sup>1,2</sup>, Karsten Parker<sup>2</sup>, Yanqiang Zhan<sup>1,2</sup>, Matthew Miller<sup>2</sup>  
and Meng-Yang Zhu<sup>2</sup> 

## Abstract

Oxidative stress-induced DNA damage has been considered to constitute a unifying pathogenesis in the development of Parkinson's disease (PD). In the present study, multiple measurement methods were applied to examine the expression of DNA damage markers in the brain of the vesicular monoamine transporter 2 transgenic mice (VMAT2 Lo), a PD animal model. The results demonstrated that mainly in the substantia nigra (SN) and locus coeruleus (LC) of VMAT2 Lo mice at the ages of 18 and 23 months, there was a significant increase in the protein levels of phosphor-ataxia telangiectasia mutated (pATM), as well as ATM and RAD 3-related (pATR) two DNA damage sensors, and  $\gamma$ -H2A histone family member X ( $\gamma$ -H2AX), a DNA damage marker of double-strand breaks (DSBs). Furthermore, these alterations were accompanied by a significant elevation of mRNA and protein levels of Cav1.2 and Cav1.3, two voltage-gated  $\text{Ca}^{2+}$  channel proteins, and modulator of calcium homeostasis in the SN and LC. Finally, the measurements of TUNEL assay and immunostaining in the brain regions confirmed the presence of apoptosis and a marked increase of immunoreactive 8-oxo-7,8-dihydro-2'-dihydroguanosine (8-OHdG) and p53-binding protein 1 (53BP1), two DNA lesion indicators induced by oxidative stress. These novel findings are coincident with the observations previously reported in PD patients and PD animal models, and provide the evidence for the features of DNA damage involved in pathogenesis of PD and feasibility of this model for investigation of PD.

## Summary Statement

The present study examined expression of DNA damage markers in VMAT2 Lo PD model mice. The results demonstrate there is a significant increase in these DNA damage markers mostly in the brain regions of 18- and 23-month-old model mice, indicating oxidative stress-induced DNA lesion is an important pathologic feature of this mouse model.

## Keywords

DNA damage,  $\gamma$ H2AX, oxidation stress, ATM/ATRdopamine, locus coeruleus, substantia nigra

Received August 5, 2022; Revised December 31, 2022; Accepted for publication January 3, 2023

## Introduction

DNA damage implies any modification of DNA resulting in changes of its coding properties and functions and is one of the important consequences following exposure to some genotoxic agents. Diverse exogenous and endogenous insults can lead to DNA damage through intracellular and extracellular processes. The exogenous insults can be exposure to cytotoxic and genotoxic agents like ionizing radiation, drugs and other chemicals (O'Neill & Wardman, 2009; McMillan et al., 2008; Ward, 1988). The endogenous sources of DNA lesion refer to replication stress and oxidative stress both of which produce free radicals from oxygen metabolism as by-products such

as reactive oxygen species (ROS) (Kryston et al., 2011). As a result of attack from free radicals, oxidant stress causes cellular damage by DNA base modifications and single- and double-strand DNA strand breaks (Temple et al., 2005).

<sup>1</sup>Department of Neurology, Renmin Hospital of the Wuhan University, Wuhan, China

<sup>2</sup>Departments of Biomedical Sciences, Quillen College of Medicine, East Tennessee State University, Johnson City, TN, USA

### Corresponding Author:

Meng-Yang Zhu, Department of Biomedical Sciences, Quillen College of Medicine, East Tennessee State University, Johnson City, TN 37604, USA.  
Email: zhum@etsu.edu



These damages can trigger DNA damage response (DDR), which is characterized by activation of sensor kinases such as ataxia-telangiectasia mutated (ATM), and ATM and Rad 3-related (ATR), formation of DNA damage foci containing phosphorylated histone H2AX ( $\gamma$ -H2AX), as well as induction of checkpoints proteins (Jackson & Bartek, 2009). These triggered DDR can also activate defense systems to counter these lesions. However, when this balance between DNA damage and DNA repair is broken, genome replication and transcription are blocked and leads to further mutations or genome aberrations of vital cellular components including DNA damage proteins and lipids (Uttara et al., 2009). While these free radicals can attack all vital cellular components like DNA, the nuclear and mitochondrial DNA damage has caught much attention, because DNA replication and transcription is blocked, leading to mutations or genome aberrations that threaten cell or organism viability, leading to the development and pathogenesis of several biological disorders (Halliwell, 1994).

The main pathologic alteration in Parkinson's disease (PD) has been considered the degeneration of a defined population of dopaminergic neurons in the brain. However, there is clearly significant neurodegeneration in the other brain regions including the locus coeruleus (LC). Dopamine (DA) has long been thought to be a risk factor for dopaminergic neurons in the brain (Meiser et al., 2013). Related to DA, long time using exogenous L-DOPA in large doses for the treatment of PD patients has negative effects due to its toxicity and metabolic influence (Dorszewska et al., 2014). Cellular oxidative stress caused by the oxidation of excess amount of DA could put these cells at risk (Miyazaki & Asanuma, 2008). Nevertheless, there must be other factors contributing to the neuronal degeneration in PD. Among these factors, oxidative DNA damage may play an important role (Merlo et al., 2016), which has a growing body of reports. For example, 8-hydroxyguanine and 8-oxo-7,8-dihydro-2'-dihydroguanosine (8-OHdG) is a biomarker of oxidative DNA damage (Emamzadeh & Surguchov, 2018; Shigenaga et al., 1989). An elevated level of 8-OHdG has been found in the substantia nigra (SN) (Shimura-Miura et al. 1999; Zhang et al., 1999) and in biological samples (Karahalil et al., 2022) of PD patients (Alam et al., 1997). Consequently, the increased levels of ROS and oxidation of macromolecules including 8-OHdG make PD patients more prone to pathologic alteration (Karahalil et al., 2022). In addition, a pronounced increase in nuclear DNA (nDNA), single-strand breaks (SSBs), and double-strand breaks (DSBs) were observed in PD brains. Western blot analysis on PD human samples showed a significant increase in  $\gamma$ -H2A histone family member X ( $\gamma$ -H2AX) protein levels, which is a recognized marker of DSBs. A significant activation of ATM, a key player in DSB repair, was also reported, indicating that the DDR could contribute to the pathogenesis of PD (Camins et al., 2010). All these findings support the hypothesis that

DNA damage induced by oxidative stress represents a key pathogenic factor in PD (Migliore et al., 2002; Migliore et al., 2001), and oxidative DNA damage could be a specific molecular marker of PD (Gonzalez-Hunt & Sanders, 2021; Merlo et al., 2016).

The neural-specific vesicular monoamine transporter 2 (VMAT2) is a transmembrane protein and is a key regulator of monoamine homeostasis by implication in monoamine storage, protection of neurotransmitters from oxidation, and control of quantal secretion of these neurotransmitters (Erickson et al., 1992). Therefore, functional failure of VMAT2 has been recognized as a contributor to the pathology of PD (Lotharius & Brundin, 2002). VMAT2 Lo is a transgenic mouse with ~95% shutdown in endogenous VMAT2 expression (Colebrooke et al., 2006; Mooslehner et al., 2001). These mice are characterized by highly dysregulated transmitter homeostasis such as DA and norepinephrine (NE), progressive neuronal degeneration and formation of  $\alpha$ -synuclein containing inclusions in the SN, with the ventral tegmental area unaffected (Caudle et al., 2007; Surguchov, 2022; Taylor et al., 2011; Taylor et al., 2009). In addition, these mice exhibited non-motor features and L-DOPA-responsive motor deficits. Therefore, this model replicated essential pathogenic characteristics of PD. While many biochemical features in these model mice have been documented, little is known about the processing of the DNA damage in these animals and no study has yet examined whether there are potential DNA damage changes involved. It is critical to explore these pathologic characteristics for the complete establishment of a useful PD model.

In the present study, we examined mRNA and protein levels of several DNA damage markers in the brain regions of VMAT2 Lo mice at different ages. Furthermore, using immunochemistry, immunofluorescence (IF) assays, and the terminal deoxynucleotidyl transferase-mediated biotinylated UTP nick end labeling (TUNEL), the changes of some DNA damage markers in brain regions were assessed. The results demonstrated that compared to controls, VMAT2 Lo mice showed an increase in protein levels of phospho-ATM (pATM) and phospho-ATR (pATR) in the frontal cortex (FC) and SN, as well Cav1.2/Cav1.3, two voltage-gated  $Ca^{2+}$  channel proteins, and modulators of calcium homeostasis, in the LC and SN. These increased protein levels in these brain regions were paralleled by a similar alteration of mRNA levels of ATM/ATR, as well as Cav1.2/Cav1.3. Furthermore, immunochemical measurements revealed elevated levels of 8-OHdG and p53-binding protein 1 (53BP1) in the related brain regions. These data demonstrate that DNA damage is a significant pathogenesis in this PD mouse model, especially when age of the mouse is also considered. This not only provides evidence for the feasibility of this PD model, but also extends our understanding of this field and may have a potential effect on PD disease-modifying therapies.

## Materials and Methods

### Animals

The present study used both male and female VMAT2 Lo mice (RRID: MGL\_3758030), courtesy of Dr. Gary Miller, Department of Environmental Health Sciences, Mailmen School of Public Health, Columbia University, New York, USA. These mice were bred in the animal facility of this university. These mice were housed on a 12-hour light/dark cycle with food and water provided *ad libitum*. All animal handling procedures followed the guide approved by the Animal Care and Use Committee of East Tennessee State University, which complies with the NIH Guide for the Care and Use of Laboratory Animals (Council 2011). In the present project, different ages of mice (2, 6, 15, 18, and 23 months) and age-matched wild-type littermates were selected and randomly assigned. A power analysis was performed to estimate the number of animals used in the groups by assuming the weaker of the two effects, which was also based on our preliminary studies. Although this study used both male and female mice, the sex of animals was not separately divided in the group. Therefore, sex-dependent effects were not assessed.

The VMAT2 Lo mice of different ages and their littermates were sacrificed in two ways based on the processing procedures. For biochemical measurements, mice were fast decapitated at the predetermined ages without anaesthetization. Brains were removed and rapidly frozen in 2-methyl-butane on dry ice, then stored at  $-80^{\circ}\text{C}$  until dissection of the brains. For TUNEL, immunostaining, and IF, transcranial perfusion using 4% paraformaldehyde in 0.1 mol/L phosphate buffer, pH 7.4, was performed on the mice under anesthesia with ketamine/xylazine (100mg/10mg/kg, i.p.). Then brains were collected and stored at  $-80^{\circ}\text{C}$  until the desired sectional cut was obtained using a Leitz 1512 microtome (Leitz Co., Germany).

### RNA Isolation and Quantitative Real-Time Polymerase Chain Reaction (qPCR) Analysis for mRNAs of *ATM*, *ATR*, and *Cav1.2/1.3* in Brain Regions

Similar methods were used for RNA isolation and qPCR analysis as described before (Fan et al., 2020). Briefly, total RNA was extracted from dissected brain regions of mice using the RNeasy reagents (Molecular Research Center, Inc., Carlsbad, CA) and converted to cDNAs by the superscript III First-Strand Synthesis Kit (Applied Biosystems/Life Technologies, Foster City, CA, USA) according to the manufacturer's protocol. The following primers were used for qPCR analysis: mouse *ATM*: 5'-TAGGCACACAGCTAGTCTTA-3' and 5'-GGAGGTGGATCTGTTAGTTC-3'; mouse *ATR*: 5'-GACACTCCAAAGC ACCACTGAA-3' and 5'-GGCAGCCCTGTTACTCTATTT CG -3'; mouse *Cav1.3*: 5'-AGAGGACCATGCGAACGAG-3' and 5'-CCTTACCAGAAATAGGGAGTCT-3'; mouse *Cav1.2*: 5'-TACAGCCTTCAAATGTGGTC-3' and 5'-ACTG ACTTCACTGAACA-3'; mouse  $\beta$ -*actin*: 5'-CAAC

GAGCGGTTCCGATG-3' and 5'-GCCACAGGATTCCATA CCCA-3'. The relative changes in gene expression from qPCR were analyzed as follows: first, the value of each gene of interest was normalized to  $\beta$ -actin ( $\Delta\text{Ct}$ ). Then comparisons of mRNA expression levels of each respective gene were calculated by taking the inverse log of  $\Delta\Delta\text{CT}$ , which resulted in the relative fold change comparative threshold cycle method ( $2^{-\Delta\Delta\text{CT}}$ ) (Livak & Schmittgen, 2001). All measurements were run in triplicate, each using a separate set of cDNA aliquot.

### IF, Immunohistochemical (IHC), and TUNEL Labeling

These methods follow similar protocols from our laboratory (Fan et al., 2011; Zhu et al., 2019). All three methods used the free-floating sections of different brain regions. For IF of 53BP1, briefly, the sections were pretreated in 5% bovine serum albumin in phosphate-buffered saline (PBS) supplemented with 0.4% Triton-X 100. Then these sections were incubated with primary antibody solution (polyclonal antibody against 53BP1, 1:1,000, NB100-304, RRID: AB\_2209928, NOVUS Biologicals, Centennial, CO, USA) overnight at  $4^{\circ}\text{C}$ . The next day, these sections were further incubated with secondary antibodies (Alexa Fluor 488-conjugated goat anti-rabbit IgG, from Abcam, Cambridge, MA, USA) after washing with 0.1 M PBS for 4 times. Then, the floating sections were mounted onto slides. IF labeling in the slides was observed and acquired in a Leica TCS SP2 confocal microscope system (Leica Microsystems Inc., Bannockburn, IL, USA), and analyzed quantitatively by ImageJ software (Rasband, US National Institutes of Health, Bethesda, <http://rsbweb.nih.gov/ij>, 2010). The reference background levels in images of brain sections adjacent to the target region were taken as non-immunoreactive portions.

For IHC of 8-OHdG and  $\gamma$ -H2AX, the brain sections were rinsed with PBS for 3 times, followed by blocking with 10% (v/v) nonimmune goat serum for 30 min. After rinsing, sections were incubated with antibodies against mouse (for 8-OHdG: polyclonal, BS-1278R, 1:200, ThermoFisher Scientific, Waltham, MA, USA, RRID: AB\_2892631; for  $\gamma$ -H2AX: polyclonal, A300-081A, 1:100, Bethyl Laboratory, Waltham, MA, USA, RRID: AB\_203288) overnight at room temperature. The next day, the sections were further exposed to biotinylated horse anti-mouse IgG. Thereafter, the sections were visualized with 3,3-diaminobenzidine (DAB) in 0.1 M Tris buffer and subsequently counterstained with hematoxylin after differentiation with hydrochloric alcohol (Vectastain; Vector Laboratories), followed by a final seal with neutral gum. The photos were captured a Leica TCS SP2 confocal microscope system (Leica Microsystems Inc., Bannockburn, IL, USA), and were analyzed quantitatively by ImageJ software (Rasband, US National Institutes of Health, Bethesda, <http://rsbweb.nih.gov/ij>, 2010).

TUNEL labeling was performed to examine the neuronal cell death in these mice. This method was based on our previous publication (Zhu et al., 2006; Zhu et al., 2019) with some modifications. This labeling used the ApopTag Fluorescein In Situ

Apoptosis Detection Kit (MilliporeSigma, Burlington, MA, USA) based on the manufacturer's protocol. Briefly, the slides were incubated in 3.0% hydrogen peroxide in PBS for 5 min at room temperature to quench endogenous peroxidase. After rinsing, the slides were briefly soaked with equilibration buffer, followed by addition of TUNEL reagents [terminal deoxynucleotidyl transferase (TdT) and digoxigenin-deoxyuridine triphosphate (dUTP) reaction buffer] and incubated in a humidified chamber at 37°C for 1 h. Then, the slides were applied with Anti-Degoxigenin Peroxidase Conjugate, and developed color peroxidase substrate by adding peroxidase substrate. Finally, these slides were counterstained with 4-6-diamidino-2-phenylindole (DAPI) as a fluorescent tracer to detect nuclei.

After covering with coverslips using Cityfluor mounting medium (Ted Pella, Inc., Redding, CA USA) and further sealing with clear nail polish, these slides were examined and photographed using an EVOS inverted fluorescent microscope (Advanced Microscopy Group, Washington, USA). TUNEL-positive cells in the images were analyzed using the multipoint selector tool in ImageJ and counted in the given interested area per millimeter square on DAB-staining images using ImageJ software (NIH; Bethesda, MD, USA).

### Western Blot Analysis:

Western blotting was performed using similar methods as to that reported previously from our laboratory (Fan et al., 2011). Briefly, equal amounts of proteins (about 30 µg) from each sample were loaded into an SDS-polyacrylamide gel (10% or 15%) and electrophoretically fractionated. Next, the proteins from the gel were electronically transferred onto polyvinylidene difluoride membranes. These membranes were respectively incubated with different primary antibodies [for  $\gamma$ -H2AX (05-636), 1:1,000, polyclonal, MilliporeSigma, Burlington, MA, USA, PRID: AB\_10002815. For mouse ATM monoclonal: MA1-23152, 1:1,000, ThermoFisher Scientific, Waltham, MA, USA, PRID: AB\_557657; for mouse pATM polyclonal rabbit: AF1655-SP, (s1981), 1:1,000, R & D Systems, Minneapolis, MN, USA, PRID: AB\_2274566; for mouse ATR: monoclonal, 1:1,000, NB100-308, Novus Biologicals, Centennial, CO USA, PRID: AB\_10000618; for mouse pATR: (Thr1989), monoclonal (HL132), 1:1000, MA5-36263, ThermoFisher Scientific, Waltham, MA, USA PRID: AB\_2722679. For Cav1.2 (MA13170), 1:1,000, MilliporeSigma, Burlington, MA, USA, PRID: AB\_2069565. For Cav1.3 (ab84811), 1:1,000, Abcam, Cambridge, MA, USA, PRID: AB\_2314104. For 53BP1, polyclonal (ab36823), 1:1,000, Abcam, Waltham, MA, USA, PRID: AB\_722497] overnight at 4°C. Then these membranes were exposed to the secondary antibody against rabbit or mouse. After washing, these membranes were further exposed to enhanced chemiluminescence (ECL, Amersham Life Sciences, Buckinghamshire, UK) or super ECL (Sigma Chemical Co., St Louis, MO, USA). G:Box Imaging (Frederick, MD, USA) was used to visualize the

immunoreactive bands. To verify the equal loading and transfer effectivities, an immunoreactive band of  $\beta$ -actin was examined via similar incubation processes after stripping the membranes of the previous protein-antibody complexes and then using a monoclonal antibody against  $\beta$ -actin (1:10,000 dilution, Amersham Life Sciences, Buckinghamshire, UK, PRID: AB\_22885189). Image J (RRID: SCR\_003070, Rasband, US National Institutes of Health, Bethesda, <http://rsbweb.nih.gov/ij>, 2010) was used to analyze the images of immunoreactive bands on the membranes.

### Statistical Analysis

All experimental data are presented in the text and graphs as the means  $\pm$  SEM, with an enumerated replicate number (N=x/group) in the figure legends. Statistical analysis was carried out using the unpaired Student's *t*-test, as there were only two groups (Ko mice and age-matched wild-type littermates as the control) to be compared in the present study. We did not compare the difference between mice at different ages.

## Results

It has been reported that starting from the age of 2 months, VMAT2 Lo mice display substantial reductions of DA levels in striatum and cortex, and significantly progressive neurodegeneration in the SN with the formation of  $\alpha$ -synuclein containing inclusions around the age of 18 months (Taylor, 2014). In this model, neuronal loss in the LC starts earlier (at 12 months, and with a larger reduction at 18 months of age) than occurs in the SN (beginning at 18 months and reaching significant degeneration at 24 months and maximal severity at 30 months), thereby replicating important features of PD (Caudle et al., 2007; Taylor et al., 2014). Therefore, in this study, VMAT2 Lo mice at different ages (2, 6, 15, 18, and 23 months) were initially selected to examine potential alteration of the DNA damage markers, and age-matched wild-type littermates were used as the control. However, except for protein levels of pATR in the FC, the measurements of western blotting, qPCR, immunohistochemistry, IF, and TUNEL labeling showed no significant changes in brain regions of VMAT2 Lo mice at the ages of 2, 6, and 15 months. Thus, only the results in mice at the ages of 18 and 23 months are presented for most data. In addition, generally, four brain regions [the FC, hippocampus (Hip), SN, and LC] were used for measurements. Nevertheless, some brain regions did not show a significant alteration for some measurements. Therefore, most presented data are from the LC and SN.

### *VMAT2 Lo mice showed an increased protein level of pATM/pATR, $\gamma$ -H2AX, and Cav1.2/Cav1.3 in the brain regions.*

There is a global signaling network called the DDR that senses different types of damage and coordinates a series of

responses such as activation of transcription, cell cycle control, and apoptosis (Zhou & Elledge, 2000). A pair of related protein kinases in the DDR, pATM, and pATR, is activated by DNA damage and is the core of the DNA damage signaling apparatus (Kastan & Bartek, 2004). First, the protein levels of pATR and ATR in the FC were measured by western blotting. As shown in Figure 1A, in the FC of VMAT2 Lo mice at 6, 15, 18, and 23 months of age, the pATR protein levels were significantly increased ( $p < .05$  or  $p < .01$ , respectively), while ATR protein levels were not significantly altered, when compared to those of controls. Similarly, protein levels of pATM and ATM were examined in these samples. While the protein levels of pATR in the SN exhibited a moderate increase in VMAT2 Lo mice at the ages of 18 and 23 months, ( $p < .05$ , Figure 1B) with a not noticeable change in ATM protein levels. Nevertheless, western blotting of the samples from other ages did not show a significant alteration (data are not shown). Furthermore, there was no significant change for pATR protein levels in the Hip and LC, either (data are not shown).

The protein measurement of another DNA damage sensor, pATM, showed a statistically significant increase in the LC of VMAT2 Lo mice at 18 and 23 months of age and in the SN of VMAT2 Lo mice at the ages of 18 and 23 months, when compared to those of the control (all  $p < .05$ , Figure 2A).  $\gamma$ -H2AX is one of the earliest indicators of DNA DSB (Temple et al., 2005). Its protein levels were also examined in these mice. As shown in Figure 2B, in the LC of VMAT2 Lo mice at the age of 18 months and in the SN of VMAT2 Lo mice at the age of 23 months, protein levels of  $\gamma$ -H2AX revealed a marked increase ( $p < .05$  and  $p < .01$ , respectively), when compared to those of controls.

Altered calcium homeostasis is now believed to be a major source of oxidative stress and this homeostasis depends upon L-type  $\text{Ca}^{2+}$  channels (LTCCs) (Williams et al., 1984). While  $\text{Ca}^{2+}$ -induced excitotoxicity has been considered an important mechanism leading to neuronal death, Cav1.2, and Cav1.3, two subunits of the LTCCs have been considered to contribute to this homeostasis (Duda et al., 2016). Therefore, as a change in the level of Cav1.2/Cav1.3 could contribute to  $\text{Ca}^{2+}$ -mediated excitotoxicity (Guzman et al., 2010; Kang et al., 2012), their alterations in this mouse model were also measured in the present study. Figure 3 presented the altered protein levels of Cav1.2 and Cav1.3 in the LC and SN measured by western blotting. In the LC and SN of VMAT2 Lo mice at the age of 23 months, Cav1.2 protein levels were considerably increased ( $p < .05$  or  $p < .01$ , respectively), when compared to those of the control (Figure 3A). Nevertheless, besides a significant increase of Cav. 1.3 protein levels in the LC of VMAT2 Lo mice at the age of 23 months, there was a marked or moderate increase of protein levels in Cav1.3 in the SN of VMAT2 Lo mice at the ages of both 18 and 23 months, when compared to those of the controls ( $p < .05$  or  $p < .01$ , respectively, Figure 3B). Similarly, there was no significant change in the protein levels of Cav1.2/

Cav1.3 in the FC and Hip at these two age groups (data are not shown).

### *VMAT2 Lo Mice had an Increased mRNA Level of ATM/ATR, and Cav1.2/Cav1.3 in the Brain Regions*

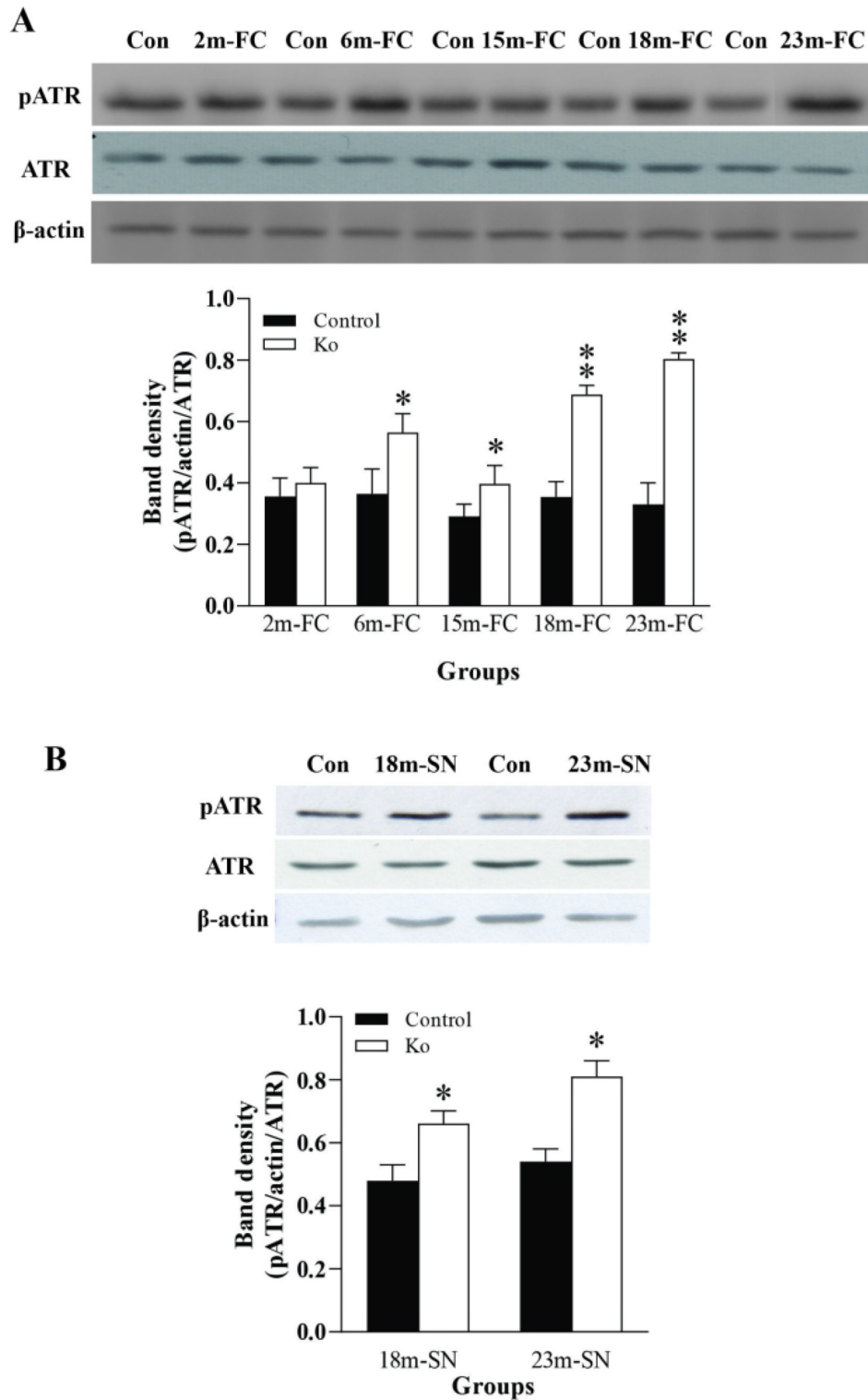
Next experiment was to examine mRNA levels of ATM, ATR, and Cav1.2/Cav1.3 in the LC and SN of these model mice as a parallel investigation. As shown in Figure 4, in the LC of VMAT2 Lo mice at 18 months of age and in the SN of VMAT2 Lo mice at 23 months of age, ATM mRNA levels were markedly increased (both  $p < .05$ ). However, such elevations were not observed in the LC at 23 months of age and in the SN of model mice at 18 months of age (Figure 4A). In the LC of VMAT2 Lo mice at both ages, and in the SN of these mice at 23 months of age there was a moderately increased ATR mRNA level (all  $p < .05$ , Figure 4B).

Figure 5A showed a significant elevation of mRNA levels of Cav1.2 in the LC of 18-month-old VMAT2 Lo mice and in the SN of these 23-month-old mice ( $p < .05$ ). However, such obviously increased Cav1.3 mRNA levels only appeared in the LC of both 18- and 23-month-old VMAT2 Lo mice (both  $p < .05$ ), not in the SN of those mice at both ages (Figure 5B). QPCR measurements did not reveal a marked alteration in mRNA levels of ATM/ATR and Cav1.2/Cav1.3 in the FC and Hip regions of VMAT2 Lo mice at both ages.

### *VMAT2 Lo mice exhibited cell damage as indicated by TUNEL staining, and elevated immunoreactivities of $\gamma$ -H2AX, 8-OHdG as well as 53BP1 in brain regions.*

The TUNEL staining was performed on these VMAT2 Lo mice to explore the oxidative stress-caused apoptosis in the brain. Sparse numbers of TUNEL labeled cells that exhibited inter-nucleosomal DNA fragmentation were found in the FC, Hip, SN, and LC of controls (top panels in Figure 6A, B, C, and D). In contrast, large numbers of TUNEL-positive cells were observed in these regions of VMAT2 Lo mice at the ages of 18 and 23 months (lower panels in Figure 6A, B, C, and D). Analysis displayed that the difference was very significant between the model and control mice ( $F_{3,26} = 19.25$ ,  $p < .01$ ; Figure 6E).

H2AX is a variant of histone H2A and a component of the histone octamer in a subset of nucleosomes. When DSBs occur, H2AX is phosphorylated to form  $\gamma$ -H2AX, which is central in the protein recruitment and signaling cascade of the DDR (Kinner et al., 2008). Thus it is used as a biomarker for DSBs and DNA damage (Ivashkevich et al., 2012). As shown in Figure 7, the immunoreactivity of  $\gamma$ -H2AX was detected in nuclei of neuronal cells. While there are some positive  $\gamma$ -H2AX staining in the control, a significantly increased immunoreactivity of  $\gamma$ -H2AX exhibited in the SN and LC of



**Figure 1.** VMAT2 Lo mice have increased protein levels of pATR in the FC (A) at the ages of 6, 15, 18, and 23 months and in the SN and (B) at the ages of 18 and 23 months (N=6/group). The upper panels in A and B show autoradiographs obtained by western blotting for pATR, ATR, and  $\beta$ -actin. The lower panels in A and B show quantitative analysis of band densities.

Note. Abbreviations: ATR=ataxia telangiectasia mutated and RAD 3-related; Con=controls; ; FC=frontal cortex; Ko=VMAT2 Lo mice; pATR=phosphor-ataxia telangiectasia mutated and RAD 3-related; SN=substantia nigra; VMAT2 Lo=vesicular monoamine transporter 2 transgenic mice; 2m, 6m, 15m, 18m, and 23m=2, 6, 15, 18, 23 month-old mice.

\* $p < .05$ , \*\* $p < .01$ , compared to the control.

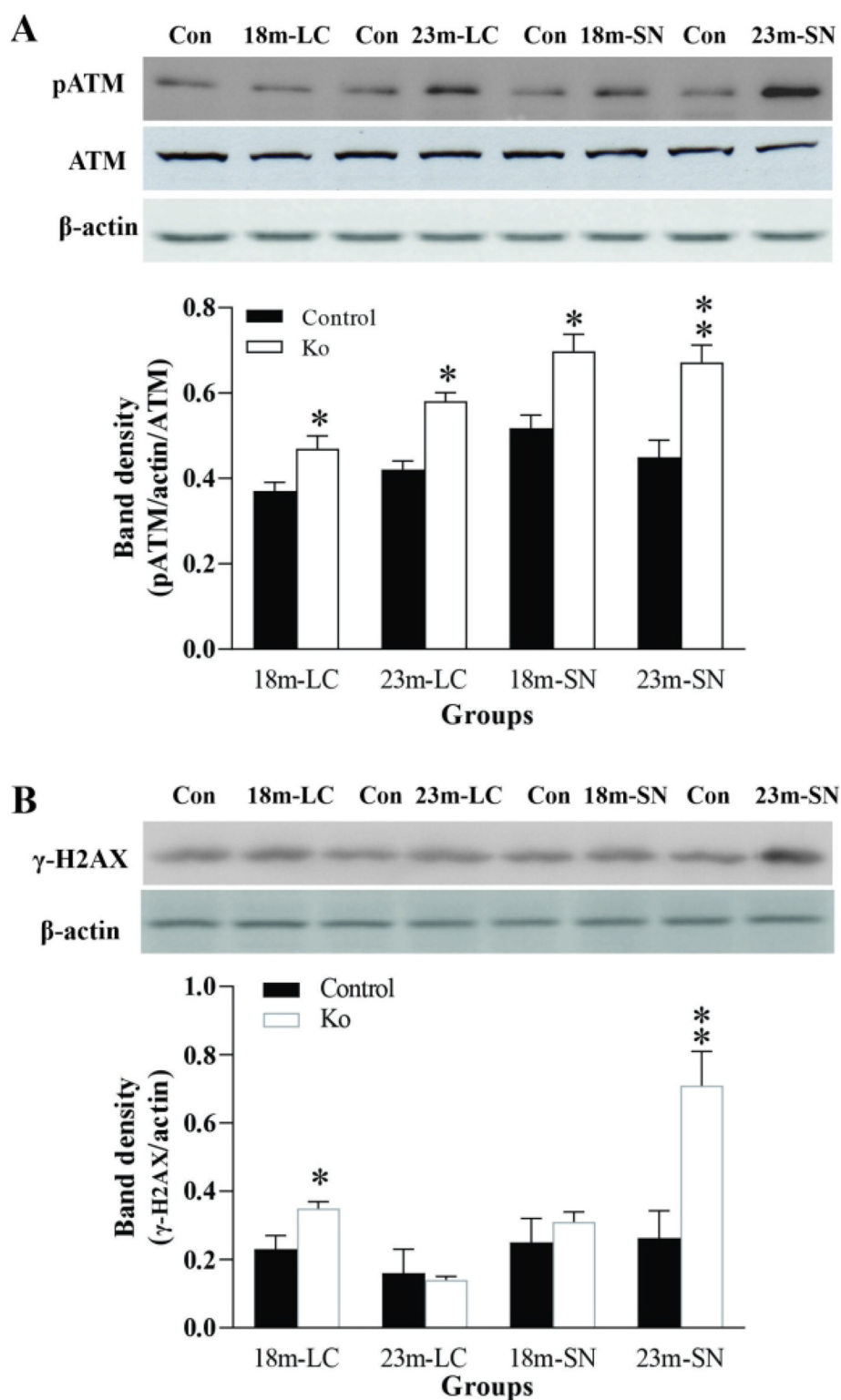


**Figure 2.** VMAT2 Lo mice have increased protein levels of pATM (A) and  $\gamma$ -H2AX (B) in the LC and SN at the ages of 18 and 23 months (N=6/group). The upper panels in A and B show autoradiographs obtained by western blotting for pATM, ATM and  $\beta$ -actin. The lower panels in A and B show quantitative analysis of band densities.

See Figure 1 for abbreviations.

\* $p < .05$ , \*\* $p < .01$ , compared to the control.

Note. ATM=ataxia telangiectasia mutated; LC=locus coeruleus; pATR=phosphor-ataxia telangiectasia mutated and RAD 3-related; SN=substantia nigra; VMAT2 Lo=vesicular monoamine transporter 2 transgenic mice;  $\gamma$ -H2AX= $\gamma$ -H2A histone family member X.

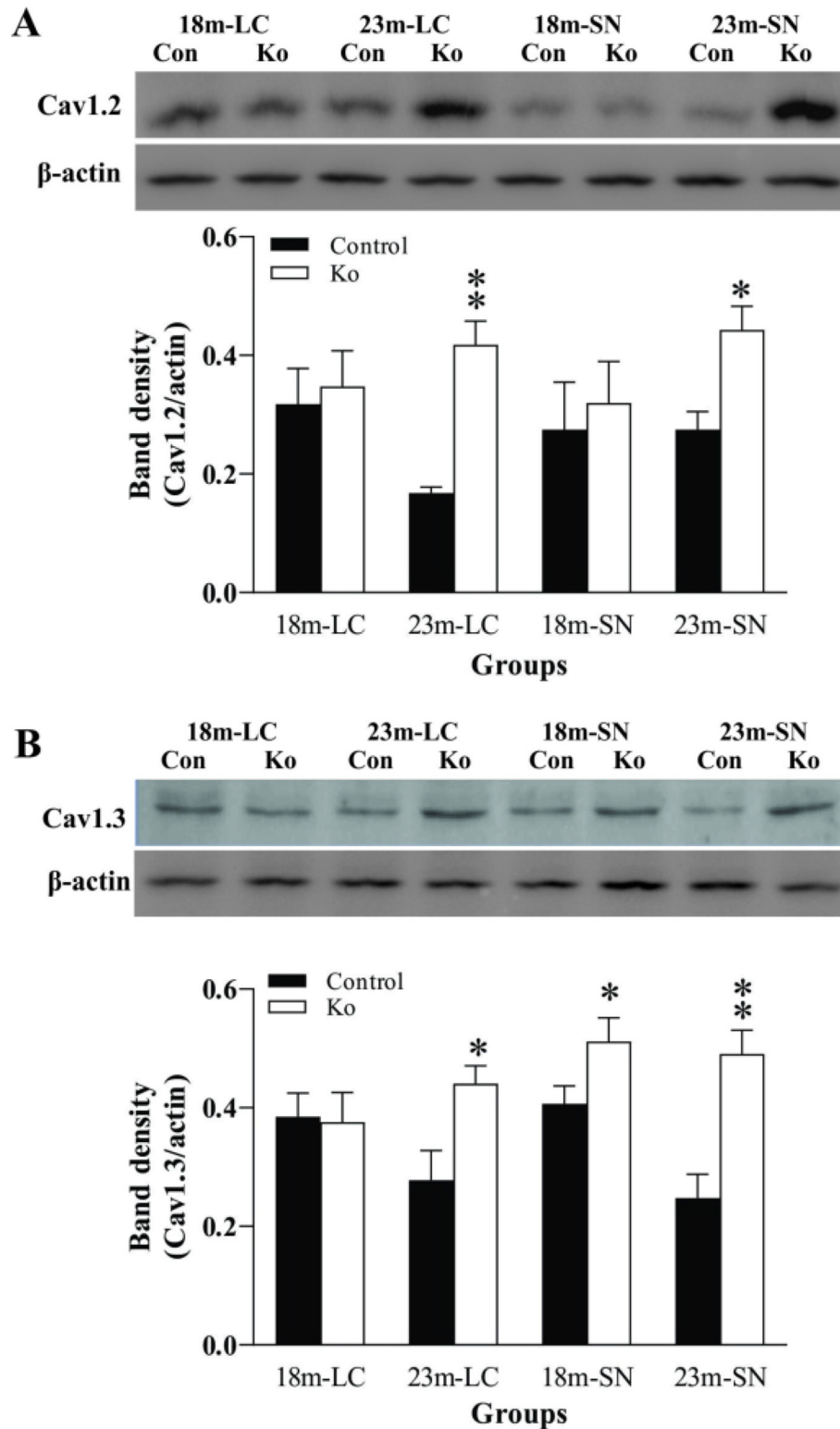


**Figure 3.** VMAT2 Lo mice have increased protein levels of Cav1.2 (A) and Cav1.3 (B) in the LC and SN at the ages of 18 and 23 months (N=7/group). The upper panels in A and B show autoradiographs obtained by western blotting. The lower panels in A and B show quantitative analysis of band densities.

See Figure 1 for abbreviations.

Note. LC=locus coeruleus; SN=substantia nigra; VMAT2 Lo=vesicular monoamine transporter 2 transgenic mice.

\* $p < .05$ , \*\* $p < .01$ , compared to the control.

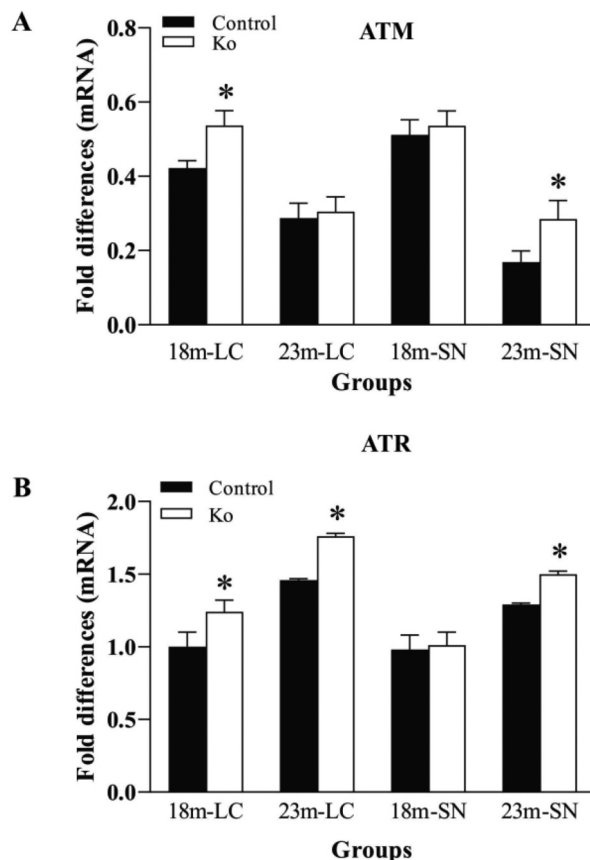


**Figure 4.** VMAT2 Lo mice have increased mRNA expression levels of ATM (A) and ATR (B) in the LC and SN at the ages of 18 and 23 months, measured by qPCR (N=5/group).

See Figure 1 for abbreviations.

Note. ATM=ataxia telangiectasia mutated; ATR=ataxia telangiectasia mutated and RAD 3-related; LC=locus coeruleus; SN: substantia nigra; qPCR=quantitative real-time polymerase chain reaction; VMAT2 Lo=vesicular monoamine transporter 2 transgenic mice.

\* $p < .05$ , \*\* $p < .01$ , compared to the control.

VMAT2 Lo mice at the ages of 18 and 23 months ( $p < .05$  and  $p < .01$ , respectively), indicating there was a severe DNA damage in these model mice. Compared to the result of  $\gamma$ -H2AX measured by western blotting (Figure 2B), IHC analysis of  $\gamma$ -H2AX seems to be more sensitive to detect DSBs.

8-OHdG is the main product of oxidation reaction of hydroxyl radicals and guanine residues in DNA and is one of the best biomarkers of DNA damage due to oxidative stress (Hu et al., 2010). IHC staining was carried out for 8-OHdG in these mice. As shown in the figures, 8-OHdG expression was observed in the nucleus and the cytoplasm of neurons, as well as glial cells. Furthermore, the relatively weak immunoreactivity for 8-OHdG was observed in the FC (Figure 8A), Hip (Figure 8B), SN (Figure 9A), and LC (Figure 9B) of controls. However, the density of 8-OHdG immunoreactivity was prominently increased in the neuronal and glia-like cells of these brain regions in both 18-and

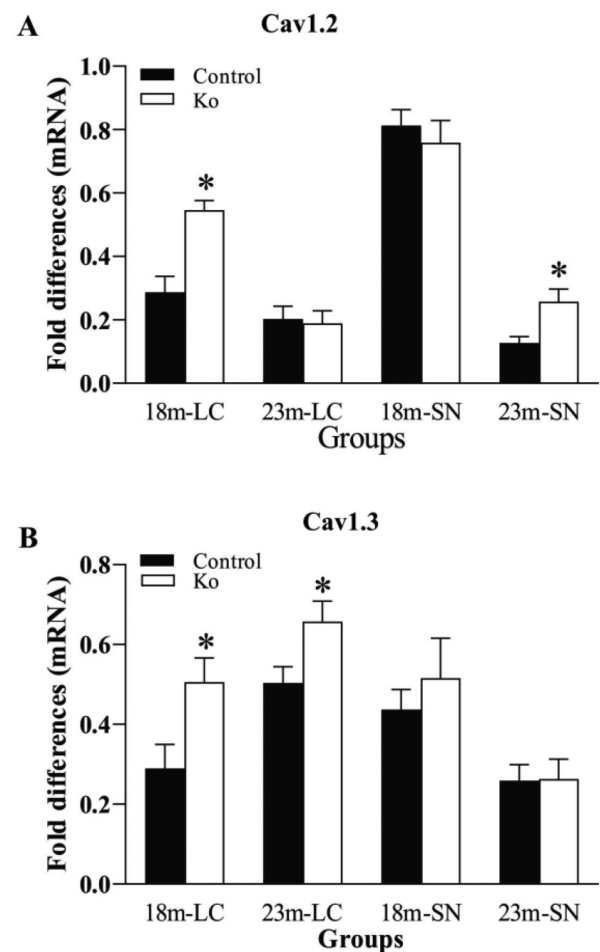


**Figure 5.** VMAT2 Lo mice have increased mRNA expression levels of Cav1.2 (A) and Cav1.3 (B) in the LC and SN at the ages of 18 and 23 months, measured by qPCR (N=7/group).

See Figure 1 for abbreviations.

Note. LC=locus coeruleus; SN=substantia nigra; qPCR=quantitative real-time polymerase chain reaction; VMAT2 Lo=vesicular monoamine transporter 2 transgenic mice.

\* $p < .05$ , \*\* $p < .01$ , compared to the control.

23-month-old VMAT2 Lo mice. Compared to those in the control, this densitometric analysis of 8-OHdG exhibited an eloquent level ( $p < .05$  or  $p < .01$ , respectively), indicating that there is obvious DNA damage.

The 53BP1 binds to the DNA-binding domain of tumor suppressor p53 and enhances p53-mediated transcriptional activation. 53BP1 is a critical transducer of the DNA damage signal and the mediator of the DNA damage checkpoint (Wang et al., 2002). Therefore, its distribution in the brain regions of VMAT2 Lo mice was measured by IF. Similarly, the results of mice at the ages of 18- and 23-month old were presented. Compared to those in the age-matched littermate controls, the immunoreactivities of 53BP1 in the FC, Hip, SN, and LC were remarkably increased (Figure 10A) in the VMAT2 Lo mice at two ages, which

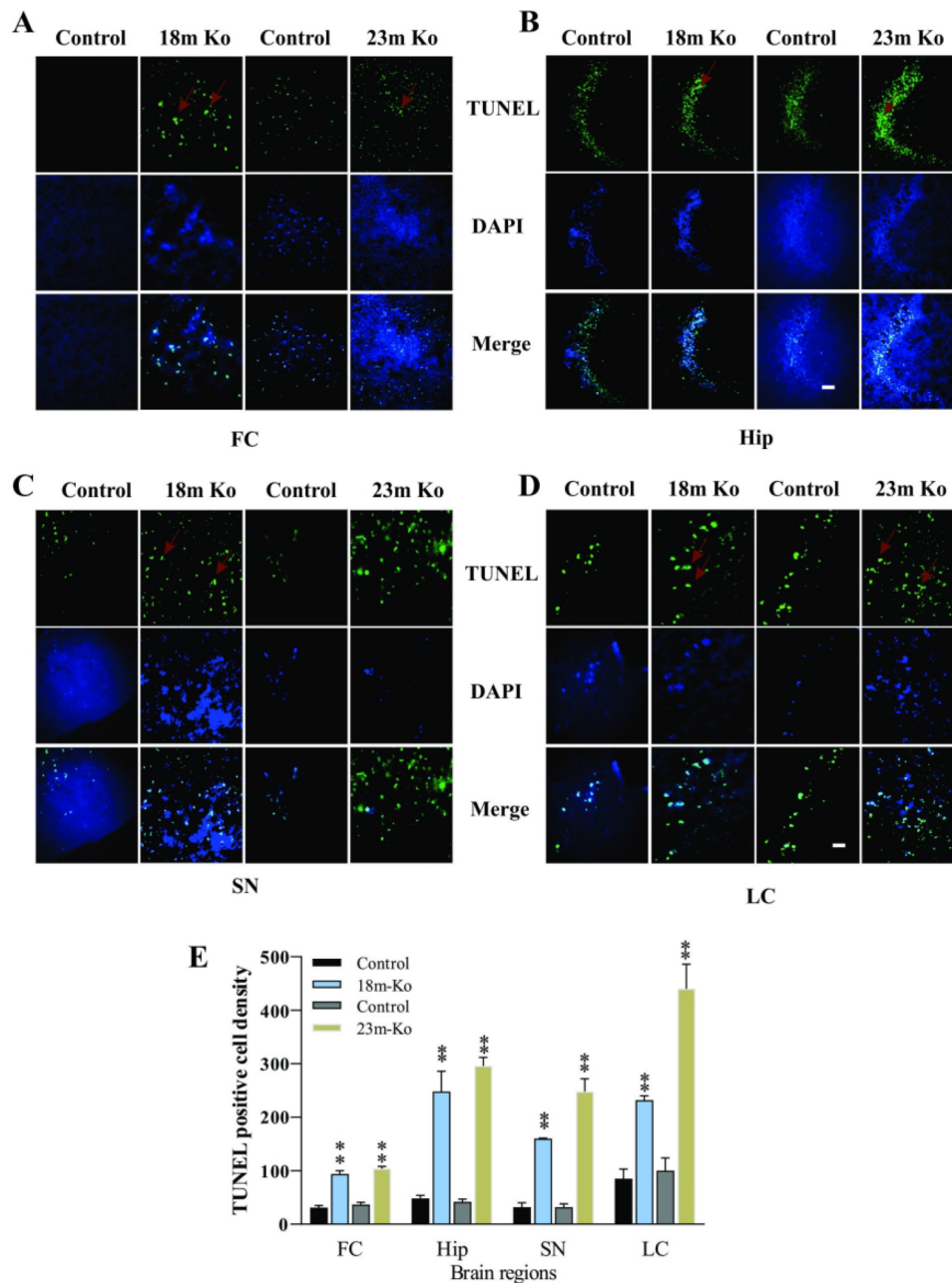


**Figure 6.** VMAT2 Lo mice exhibited apoptosis in the FC (A), Hip (B), SN (C), and LC (D), measured by TUNEL staining. Note. Data were expressed as means  $\pm$  SEM (N=4/group). TUNEL: green and DAPI: blue. E: Subsequent quantification analysis, \*\* $p < 0.01$ , compared to the control. Red arrows: point to apoptotic cells in figures. Abbreviations: DAPI=4',6-diamidino-2-phenylindole; FC=frontal cortex; Hip=hippocampus; SN=substantia nigra; TUNEL=terminal deoxynucleotidyl transferase-mediated biotinylated UTP nick end labeling; VMAT2 Lo=vesicular monoamine transporter 2 transgenic mice; 18m Ko or 23m Ko=VMAT2 Lo mice at the ages of 18 or 23 months.

was confirmed by quantitative fluorescence image analysis ( $p < .05$  or  $p < .01$ , respectively, Figure 10B).

The 53BP1 expression was parallel measured by western blotting. The results showed a statistically significant increase of 53BP1 proteins in the FC, Hip, SN, and LC of VMAT2 Lo mice at the ages of 18 and 23 months when compared to those of the control (all  $p < .05$  or  $p < .01$ , respectively, Figure 11).

## Discussion

In this article, we describe experiments that investigated the alteration of DNA damage markers in the brain regions of VMAT2 Lo mice and controls. The results showed the expression of DNA damage sensors pATR and pATM, as well as DDR marker  $\gamma$ -H2AX was significantly elevated in

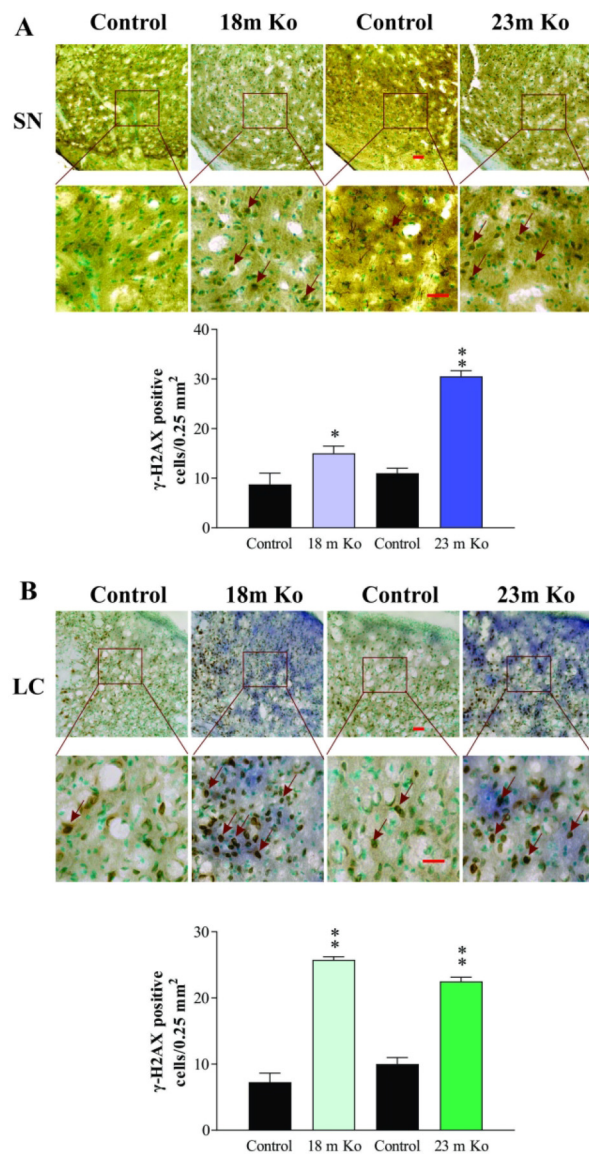


**Figure 7.** VMAT2 Lo mice showed the immunoreactive expression levels of  $\gamma$ -H2AX in the SN (A) and LC (B) compared with that in age-matched controls, as determined by immunohistochemical (IHC) analysis (N = 5/group). Upper panels in A and B: Representative images of IHC staining, red arrows indicate positive  $\gamma$ -H2AX expression. Lower panels in A and B: Subsequent quantification. Red arrows depict the positive  $\gamma$ -H2AX immunoreactivity in nuclei of cells. Scale bar= 25  $\mu$ m. Note. The values are presented as means  $\pm$  SEM. See Figure 6 for abbreviation. LC=locus coeruleus; SN=substantia nigra; VMAT2 Lo=vesicular monoamine transporter 2 transgenic mice;  $\gamma$ -H2AX= $\gamma$ -H2A histone family member X. \* $p$ <0.05, \*\* $p$  < .01 versus the control group.

brain regions, especially in the SN and LC, of VMAT2 Lo mice. Furthermore, the expressional levels of two subunits of the LTCCs, Cav1.2, and Cav1.3 were parallel increased in these brain regions. Moreover, immunochemistry, IF, and TUNEL labeling revealed an increased immunoreactive

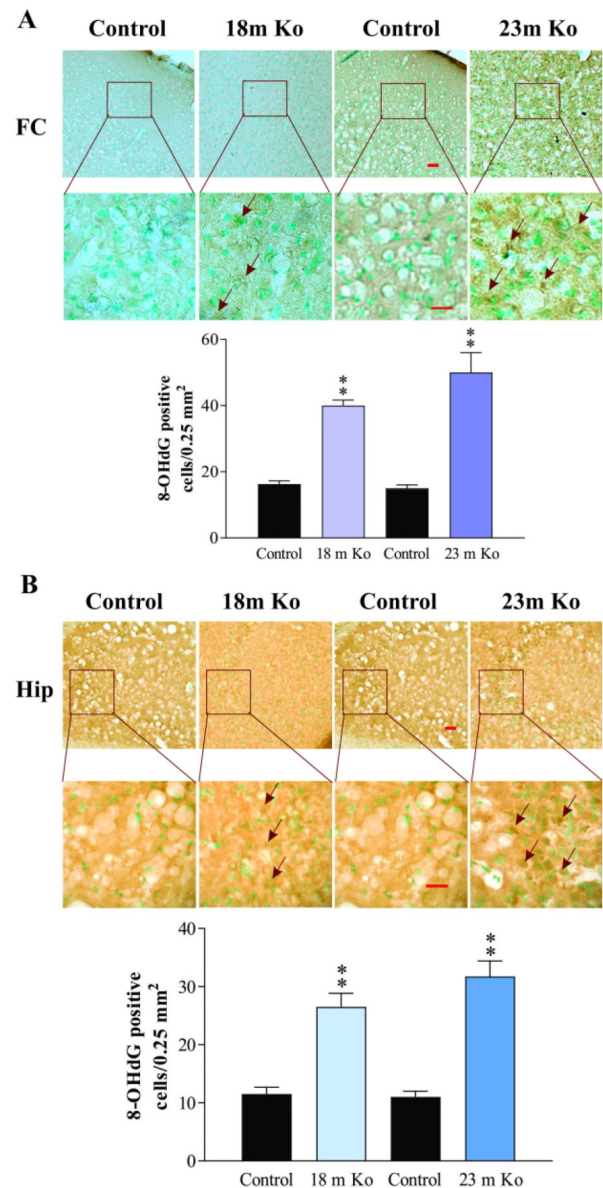


**Figure 8.** VMAT2 Lo mice showed the immunoreactive expression levels of 8-OHdG in the FC (A) and Hip (B) compared with that in age-matched controls, as determined by immunohistochemical (IHC) analysis (N = 5/group). Upper panels in A and B: Representative images of IHC staining; red arrows indicate positive 8-OHdG expression, some of which also appeared to be localized in neuronal cytoplasm. Lower panels in A and B: Subsequent quantification. Scale bar= 25  $\mu$ m. Note. The values are presented as means  $\pm$  SEM. See Figure 6 for abbreviation. FC=frontal cortex; Hip=hippocampus; VMAT2 Lo=vesicular monoamine transporter 2 transgenic mice; 8-OHdG=8-oxo-7,8-dihydro-2'-dihydroguanosine. \*\* $p$  < .01 versus control group.

$\gamma$ -H2AX, 8-OHdG, and 53BP1, as well as a marked TUNEL-positive lesion in these brain regions. These measurement results demonstrated that in these model mice, oxidative stress-caused DNA damage is a significant pathogenic

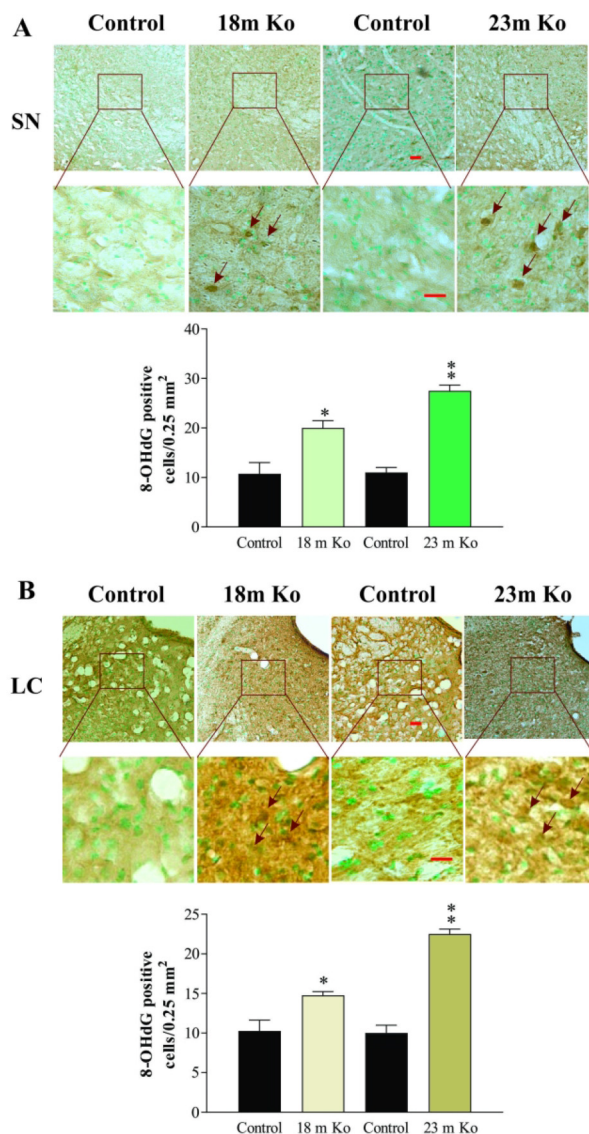


**Figure 9.** VMAT2 Lo mice showed the immunoreactive expression levels of 8-OHdG in the SN (A) and LC (B) compared with that in age-matched controls, as determined by immunohistochemical (IHC) analysis (N = 5/group). Upper panels in A and B: Representative images of IHC staining, red arrows indicate positive 8-OHdG expression, some of which also appeared to be localized in neuronal cytoplasm. Lower panels in A and B: Subsequent quantification. Scale bar = 25  $\mu$ m.

Note. The values are presented as means  $\pm$  SEM. See Figure 6 for abbreviation. LC=oculus coeruleus; SN: substantia nigra; VMAT2 Lo=vesicular monoamine transporter 2 transgenic mice; 8-OHdG=8-oxo-7,8-dihydro-2'-dihydroguanosine.

\* $p < .05$ , \*\* $p < .01$  versus the control group.

alteration. Further exploration of this exciting field in this model may elucidate the mechanisms of pathogenesis in PD. Because exploration of the new and reliable biomarkers of PD can eventually lead to the development of new treatment strategies (Enogieru et al., 2021), those manipulations such as using of inhibitor of DNA damage targeting the

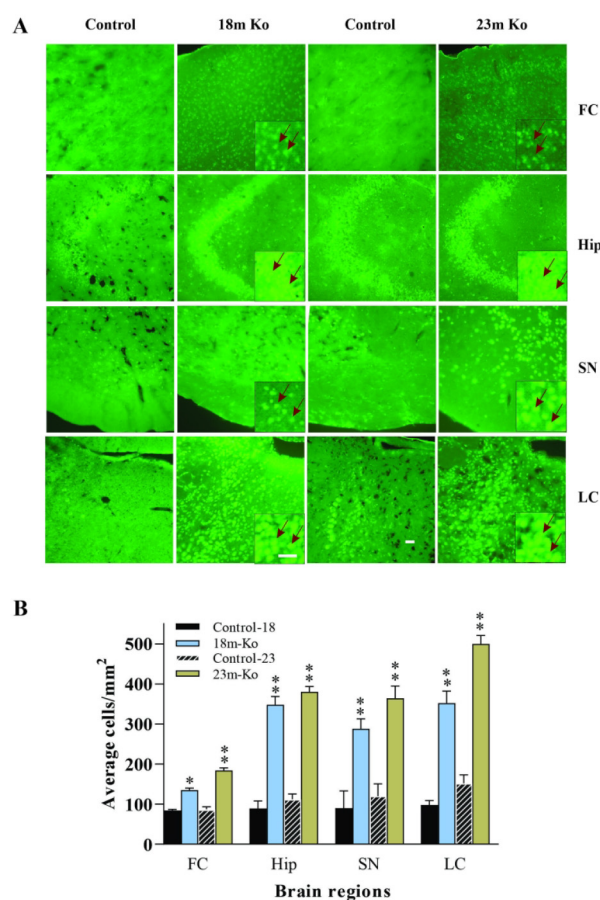


**Figure 10.** VMAT2 Lo mice showed the immunoreactive expression levels of 53BP1 (A) in the FC, Hip, SN, and LC, compared with that in age-matched controls, as determined by immunofluorescence (IF) analysis (n = 5/group). B: The graph represents 53BP1 total intensity. Representative photomicrographs of 53BP1 immunostaining. Representative IF staining to identify 53BP1-positive cells in the figures (green). The inserts on the figures of 18m and 23m Ko mice are magnified from the same figure to clarify the increased immunoreactivity (pointed by red arrows). Scale bars in figures and inserts = 25  $\mu$ m. See Figure 6 for abbreviation.

Note. FC=frontal cortex; Hip=hippocampus; IF=immunofluorescence; SN=substantia nigra; VMAT2 Lo=vesicular monoamine transporter 2 transgenic mice; 53BP-1=p53-binding protein 1.

\* $p < .05$ , \*\* $p < .01$  versus the control group.

activation of DDR have potential intervention for the treatment of PD.

It has been reported that at 2 months of age, VMAT2 Lo mice showed substantial reductions in striatal DA and cortical DA/NE levels. Neuronal loss in the LC starts at 12 months with a larger reduction at 18 months of age. Similar neuronal loss in the SN begins at 18 months, reaching significant degeneration at 24 months of age (Taylor et al., 2014). The metabolisms of amine transmitters bear a particular relevance to a cytosolic milieu that favors an oxidative state, as unprotected DA, NE, and other amines can be oxidized in the

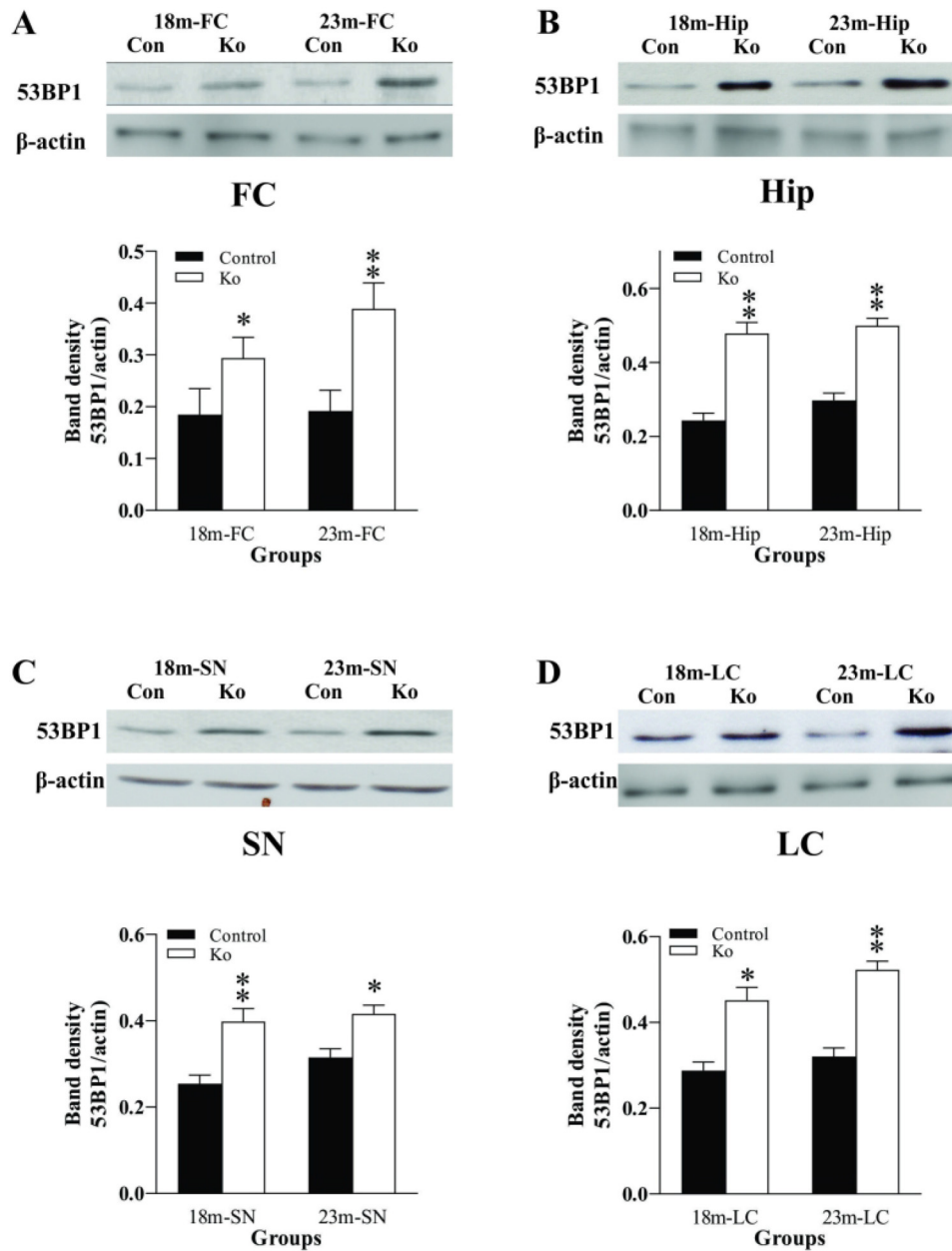


**Figure 11.** VMAT2 Lo mice have increased protein levels of 53BP1 in the FC (A), Hip (B), SN (C), and LC (D) at 18 and 23 months of age (N=6/group). The upper panels in A, B, C, and D show autoradiographs obtained by western blotting. The lower panels in A, B, C, and D show quantitative analysis of band densities. See Figure 1 for abbreviations.

Note. FC=frontal cortex; Hip=hippocampus; LC=locus coeruleus; SN=substantia nigra; VMAT2 Lo=vesicular monoamine transporter 2 transgenic mice; 53BP-1=p53-binding protein 1.

\* $p < .05$ , \*\* $p < .01$ , compared to the control.

presence of transition metals to yield ROS leading to DNA damage (Cohen, 1987; Zhang et al., 1999). This is the original reason why the different brain regions from VMAT2 Lo mice at different ages were selected to test the potential DNA damage caused by oxidative stress. However, one outcome contrasts with our expectations. That is, the remarkable alterations of most DNA damage markers are age-selective and did not show in all tested regions. For example, except for a

significant increase of pATR protein levels in the FC of VMAT2 Lo mice at all tested ages (2, 6, 15, 18, and 23), other measurements only showed similar changes in this mouse model at the ages of 18 and 23 months. There may be several possible explanations for this phenomenon. First, it may be related to the efficiency of DNA repair occurring in younger model mice. Generally, cells have developed a network of DNA repair system to counteract the harmful

effects of DNA damage, wherein each corrects a different subset of lesions. Efficient repair of damaged DNA can maintain cellular homeostasis (Flint et al., 2007). Therefore, although in those VMAT2 Lo mice at a relatively younger age, the oxidative stress was triggered by the massive production of DA and other amines occurs, and this harmful insult-induced DNA damage was compensated with multiple repair mechanisms. The second explanation may be related to a fact that DNA damage is age-associated. It is known there are age-dependent increases in oxidative damage to DNA, lipid, and proteins (Mecocci et al., 1999). For example, a study using rats demonstrated that the levels of 8-OHdG in the mitochondrial DNA of 23 months old are 12-fold higher than 6 months (Hudson et al., 1998). Other studies also revealed a similar age-associated change in 8-OHdG content in animals (Braidy et al., 2011; Helbock et al. 1998; Souza-Pinto et al., 1999) and in human (Mecocci et al., 1999). A similar observation is that a highly significant increase in phosphorylated H2AX occurs with increasing age (Massudi et al., 2012). It may be due to a difference in the activation of DNA damage checkpoint signaling in response to insults (Kim et al., 2011). Therefore, our present findings are in line with the observation that neuronal loss in the LC of VMAT2 Lo mice exhibited a larger reduction at 18 months of age and those in the SN reached significant degeneration at 24 months of age (Caudle et al., 2007; Taylor et al., 2014).

As to the region-selective alteration for DNA damage markers, one explanation may be related to the methodology sensitivity. In the present study, all IHC assays exhibited an altered expression of  $\gamma$ -H2AX, 8-OHdG, 53BP1, and positive TUNEL labels in all selected regions, but western blotting and qPCR did not. These results may be consistent with the general opinion that TUNEL labeling and immunoreactivity assays are very sensitive and specific to protein identification (Gallo et al., 1986; Gimenez-Bachs et al., 2012; Kiptoo et al., 2004), although there is a differing opinion. As to the explanation why altered protein levels of pATR only appeared in the FC of VMAT2 Lo mice at all measured ages may be related to the susceptibility of the FC to oxidative stress. The FC is a very sensitive brain region to oxidative stress (Zlatkovic et al., 2014). It was reported that stress activated the glutamatergic system in the FC more intensely than in other regions (Gilad et al., 1990; Karreman & Moghaddam, 1996), and cell degeneration and cell death is generally more severe in the FC (Coleman & Flood, 1987). Similar reports can be found in Alzheimer's disease patients that there are an approximately twofold higher level of DNA damage in the cortex when compared to controls (Mullaart et al., 1990), with a reduction in cerebral DNA repair capacity (Shao et al., 2008; Weissman et al., 2007). Furthermore, in postmortem brains of these patients, multiple oxidized bases are found in significantly higher quantities in the frontal, parietal, and temporal lobes than in control brains, with the temporal lobe being the most damaged region (Wang et al., 2005).

Nevertheless, a paradoxical finding is that we did not observe a marked alteration in the FC for some markers by western blotting and qPCR. This remains to be further addressed experimentally.

In the present study, immunochemistry of  $\gamma$ -H2AX, 8-OHdG, and 53BP1, as well as TUNEL staining was performed. 8-OHdG is considered a marker of ROS-induced oxidative damage to DNA (Valavanidis et al., 2009), and is a product of oxidative DNA damage produced by specific enzymatic cleavage after 8-hydroxylation of the guanine base (Hu et al., 2010). Our results showed a remarkable increase of positive 8-OHdG immunoreactivity in the FC, Hip, SN, and LC of VMAT2 Lo mice. To the best of our knowledge, it is the first time that immunoreactive 8-OHdG in the brain of a PD animal model has been described. This result is in agreement with reported data measured in human PD patients. It was reported that 8-OHdG levels were significantly higher than normal controls as measured in samples of urinary (Sato et al., 2005), cerebrospinal fluid (Gmitterova et al., 2009; Isobe et al., 2010), and serum (Garcia-Moreno et al., 2013) from PD patients by enzyme-linked immunosorbent assay (ELISA) or other methods. In addition, 8-OHdG concentrations are elevated selectively in the SN of PD patients using Gas chromatography/mass spectrometry (Alam et al., 1997). 53BP1 is also an indicator of DNA damage and participates in the early DDR (Anderson et al., 2001; Rappold et al., 2001; Schultz et al., 2000). Furthermore, this protein quickly relocalizes to a number of nuclear foci in response to DNA damage (Anderson et al., 2001). An important characteristic is the mutual interaction of 53BP1 and other DNA damage markers. 53BP1 has been considered the downstream effector of pATM. After relocalization at sites of DNA strand break, this protein is regulated by pATM and physically interacts with  $\gamma$ -H2AX (Rappold et al., 2001). In the present study, 53BP1 positive cells were remarkably increased in the SN and LC of VMAT2 Lo mice at the ages of 18 and 23 months (Figure 9), where protein levels of pATM and  $\gamma$ -H2AX were also increased. Our investigation is in line with the literature. It was reported that immunoreactivity of 53BP1, together with  $\gamma$ -H2AX and pATM, was significantly increased in dopaminergic neurons of AAV-synucleinopathy models of PD (Milanese et al., 2018). In addition, the immunoreactivity of 53BP1 and  $\gamma$ -H2AX foci was significantly higher in the striatum of  $\alpha$ -synuclein transgenic mouse model of PD, (El-Saadi et al., 2022; Wang et al., 2016). Taken together, these results provide evidence for the feasibility of this model.

Disturbed calcium homeostasis has been viewed as an early feature of the pathogenesis of PD. The voltage-gated  $Ca^{2+}$  channels are essential regulators of the intracellular  $Ca^{2+}$  homeostasis. While increased intracellular  $Ca^{2+}$  has been linked to the formation of ROS (Orrenius et al., 2003), the LTCCs play an important role to modulate calcium ion influx into the cells (Casamassima et al., 2010). As two subtypes of LTCCs, Cav1.2, and Cav1.3 are thought to serve

predominantly as the modulators of  $\text{Ca}^{2+}$  homeostasis in the neuronal system, especially in the SN and LC (Olson et al., 2005). Therefore, their alterations in VMAT2 Lo mice have been examined in the present study as a paralleling project. Our results showed that mRNA and protein levels of Cav1.2 and Cav1.3 were profoundly elevated in the SN and LC of VMAT2 Lo mice at the ages of 18- and 23 months. While highly activated Cav1.3 has been considered to induce higher entry of  $\text{Ca}^{2+}$  in noradrenergic and dopaminergic neurons where an oxidative stress is triggered (Hurley et al., 2013), our findings from this mouse model are comparable to the literature (Chan et al., 2007). It was reported that higher levels of Cav1.3 were reported in the LC of PD (Hurley et al., 2013), which even precedes other PD pathologic alterations (Hurley et al., 2015), and seriously influences oxidative stress responses (Sanchez-Padilla et al., 2014). Given a pathogenic role for Cav1.3 in PD, Cav1.3 may therefore represent a disease-modifying (neuroprotective) therapeutic target (Gudala et al., 2015; Lang et al., 2015).

In conclusion, in the present study, different methods were used to examine the alteration of different DNA damage markers in VMAT2 Lo PD model mice. The results showed that there is an upregulation of these biomarkers (p-ATM, pATR,  $\gamma$ -H2AX, 8-OHdG, and 53-BP1) in the different brain regions. DNA damage-induced apoptotic cell death was confirmed by TUNEL assay. Furthermore, the mRNA and protein levels of Cav1.2 and Cav1.3, two LTCC subunits were significantly elevated in these brain regions of the model mice. As we did not assess sex-dependent effects in the present study, there is no conclusion about this issue. Collectively, these data underscore the importance of DNA damage in the initiation and progress of pathogenesis of PD and feasibility of VMAT2 Lo mice in the investigation of this disease.

## ORCID iD

Meng-Yang Zhu  <https://orcid.org/0000-0002-5403-1270>

## Declaration of Conflicting Interests

The author(s) declared no potential conflicts of interest with respect to the research, authorship, and/or publication of this article.

## Funding

The author(s) disclosed receipt of the following financial support for the research, authorship, and/or publication of this article: This work was supported by the grant to Zhu MY from the National Institutes of Health (NIH) (grant number AG055107).

## References

- Alam, Z. I., Jenner, A., Daniel, S. E., Lees, A. J., Cairns, N., Marsden, C. D., Jenner, P., & Halliwell, B. (1997). Oxidative DNA damage in the parkinsonian brain: An apparent selective increase in 8-hydroxyguanine levels in substantia nigra. *Journal of Neurochemistry*, *69*(9), 1196–1203. <https://doi.org/10.1046/j.1471-4159.1997.69031196.x>
- Anderson, L., Henderson, C., & Adachi, Y. (2001). Phosphorylation and rapid relocalization of 53BP1 to nuclear foci upon DNA damage. *Molecular and Cellular Biology*, *21*(5), 1719–1729. <https://doi.org/10.1128/MCB.21.5.1719-1729.2001>
- Braidy, N., Guillemin, G. J., Mansour, H., Chan-Ling, T., Poljak, A., & Grant, R. (2011). Age related changes in NAD<sup>+</sup> metabolism oxidative stress and Sirt1 activity in wistar rats. *PLoS one*, *6*(4), e19194. <https://doi.org/10.1371/journal.pone.0019194>
- Camins, A., Pizarro, J. G., Alvira, D., et al. (2010). Activation of ataxia telangiectasia muted under experimental models and human Parkinson's disease. *Cellular and Molecular Life Sciences*, *6*(22), 3865–3882. <https://doi.org/10.1007/s00018-010-0408-5>
- Casamassima, F., Hay, A. C., Benedetti, A., Lattanzi, L., Cassano, G. B., & Perlis, R. H. (2010). L-type calcium channels and psychiatric disorders: A brief review. *American Journal of Medical Genetics Part B: Neuropsychiatric Genetics*, *153B*(8), 1373–1390. <https://doi.org/10.1002/ajmg.b.31122>
- Caudle, W. M., Richardson, J. R., Wang, M. Z., et al. (2007). Reduced vesicular storage of dopamine causes progressive nigrostriatal neurodegeneration. *Journal of Neuroscience*, *27*(30), 8138–8148. <https://doi.org/10.1523/JNEUROSCI.0319-07.2007>
- Chan, C. S., Guzman, J. N., Ilijic, E., Mercer, J. N., Rick, C., Tkatch, T., Meredith, G. E., & Surmeier, D. J. (2007). 'Rejuvenation' protects neurons in mouse models of Parkinson's disease. *Nature*, *447*(7148), 1081–1086. <https://doi.org/10.1038/nature05865>
- Cohen, G. (1987). Monoamine oxidase, hydrogen peroxide, and Parkinson's disease. *Advances in Neurology*, *45*(1), 119–125.
- Colebrooke, R. E., Humby, T., Lynch, P. J., McGowan, D. P., Xia, J., & Emson, P. C. (2006). Age-related decline in striatal dopamine content and motor performance occurs in the absence of nigral cell loss in a genetic mouse model of Parkinson's disease. *European Journal of Neuroscience*, *24*(9), 2622–2630. <https://doi.org/10.1111/j.1460-9568.2006.05143.x>
- Coleman, P. D., & Flood, D. G. (1987). Neuron numbers and dendritic extent in normal aging and Alzheimer's disease. *Neurobiology of Aging*, *8*(6), 521–545. [https://doi.org/10.1016/0197-4580\(87\)90127-8](https://doi.org/10.1016/0197-4580(87)90127-8)
- Council, N. R. (2011). *Guide for the Care and Use of Laboratory Animals*. National Academies Press.
- Dorszewska, J., Prendecki, M., Lianeri, M., & Kozubski, W. (2014). Molecular effects of L-dopa therapy in Parkinson's disease. *Current Genomics*, *1*(1), 11–17. <https://doi.org/10.2174/1389202914666131210213042>
- Duda, J., Potschke, C., & Liss, B. (2016). Converging roles of ion channels, calcium, metabolic stress, and activity pattern of substantia nigra dopaminergic neurons in health and Parkinson's disease. *Journal of Neurochemistry*, *139*(Suppl 1), 156–178. <https://doi.org/10.1111/jnc.13572>
- El-Saadi, M. W., Tian, X., Grames, M., et al. (2022). Tracing brain genotoxic stress in Parkinson's disease with a novel single-cell genetic sensor. *Science Advances*, *8*(15), eabd1700. <https://doi.org/10.1126/sciadv.abd1700>
- Emamzadeh, F. N., & Surguchov, A. (2018). Parkinson's disease: Biomarkers, treatment, and risk factors. *Frontiers in Neuroscience*, *12*, 612. <https://doi.org/10.3389/fnins.2018.00612>
- Enogieru, A. B., Haylett, W., Hiss, D., & Ekpo, O. (2021). Inhibition of gammaH2AX, COX-2 and regulation of antioxidant enzymes in MPP(+)-exposed SH-SY5Y cells pre-treated with rutin. *Metabolic Brain Disease*, *36*(7), 2119–2130. <https://doi.org/10.1007/s11011-021-00746-z>

- Erickson, J. D., Eiden, L. E., & Hoffman, B. J. (1992). Expression cloning of a reserpine-sensitive vesicular monoamine transporter. *Proceedings of the National Academy of Sciences*, *89*(22), 10993–10997. <https://doi.org/10.1073/pnas.89.22.10993>
- Fan, Y., Huang, J., Duffourc, M., Kao, R. L., Ordway, G. A., Huang, R., & Zhu, M. Y. (2011). Transcription factor Phox2 upregulates expression of norepinephrine transporter and dopamine beta-hydroxylase in adult rat brains. *Neuroscience*, *192*(1), 37–53. <https://doi.org/10.1016/j.neuroscience.2011.07.005>
- Fan, Y., Zeng, F., Brown, R. W., Price, J. B., Jones, T. C., & Zhu, M. Y. (2020). Transcription Factors Phox2a/2b Upregulate Expression of Noradrenergic and Dopaminergic Phenotypes in Aged Rat Brains. *Neurotoxicity research*, *38*(3), 793–807.
- Flint, M. S., Baum, A., Chambers, W. H., & Jenkins, F. J. (2007). Induction of DNA damage, alteration of DNA repair and transcriptional activation by stress hormones. *Psychoneuroendocrinology*, *32*(5), 470–479. <https://doi.org/10.1016/j.psyneuen.2007.02.013>
- Gallo, D., Diggs, J. L., Shell, G. R., Dailey, P. J., Hoffman, M. N., & Riggs, J. L. (1986). Comparison of detection of antibody to the acquired immune deficiency syndrome virus by enzyme immunoassay, immunofluorescence, and western blot methods. *Journal of Clinical Microbiology*, *23*(6), 1049–1051. <https://doi.org/10.1128/jcm.23.6.1049-1051.1986>
- Garcia-Moreno, J. M., Martin de Pablos, A., Garcia-Sanchez, M. I., Mendez-Lucena, C., Damas-Hermoso, F., Rus, M., Chacon, J., & Fernandez, E. (2013). May serum levels of advanced oxidized protein products serve as a prognostic marker of disease duration in patients with idiopathic Parkinson's disease? *Antioxidants & Redox Signaling*, *18*(11), 1296–1302. <https://doi.org/10.1089/ars.2012.5026>
- Gilad, G. M., Gilad, V. H., Wyatt, R. J., & Tizabi, Y. (1990). Region-selective stress-induced increase of glutamate uptake and release in rat forebrain. *Brain Research*, *525*(2), 335–338. [https://doi.org/10.1016/0006-8993\(90\)90886-G](https://doi.org/10.1016/0006-8993(90)90886-G)
- Gimenez-Bachs, J. M., Salinas-Sanchez, A. S., Serrano-Oviedo, L., Nam-Cha, S. H., Rubio-Del Campo, A., & Sanchez-Prieto, R. (2012). Carbonic anhydrase IX as a specific biomarker for clear cell renal cell carcinoma: Comparative study of western blot and immunohistochemistry and implications for diagnosis. *Scandinavian Journal of Urology and Nephrology*, *46*(5), 358–364. <https://doi.org/10.3109/00365599.2012.685493>
- Gmitterova, K., Heinemann, U., Gawinecka, J., Varges, D., Ciesielczyk, B., Valkovic, P., Benetin, J., & Zerr, I. (2009). 8-OHdG In cerebrospinal fluid as a marker of oxidative stress in various neurodegenerative diseases. *Neurodegenerative Diseases*, *6*(5-6), 263–269. <https://doi.org/10.1159/000237221>
- Gonzalez-Hunt, C. P., & Sanders, L. H. (2021). DNA Damage and repair in Parkinson's disease: Recent advances and new opportunities. *Journal of Neuroscience Research*, *99*(1), 180–189. <https://doi.org/10.1002/jnr.24592>
- Gudala, K., Kanukula, R., & Bansal, D. (2015). Reduced risk of Parkinson's disease in users of calcium channel blockers: A meta-analysis. *International Journal of Chronic Diseases*, *2015*(697404), 1–7. <https://doi.org/10.1155/2015/697404>
- Guzman, J. N., Sanchez-Padilla, J., Wokosin, D., Kondapalli, J., Ilijic, E., Schumacker, P. T., & Surmeier, D. J. (2010). Oxidant stress evoked by pacemaking in dopaminergic neurons is attenuated by DJ-1. *Nature*, *468*(7324), 696–700. <https://doi.org/10.1038/nature09536>
- Halliwell, B. (1994). Free radicals, antioxidants, and human disease: Curiosity, cause, or consequence? *The Lancet*, *344*(8924), 721–724. [https://doi.org/10.1016/S0140-6736\(94\)92211-X](https://doi.org/10.1016/S0140-6736(94)92211-X)
- Helbock, H. J., Beckman, K. B., Shigenaga, M. K., Walter, P. B., Woodall, A. A., Yeo, H. C., & Ames, B. N. (1998). DNA Oxidation matters: The HPLC-electrochemical detection assay of 8-oxo-deoxyguanosine and 8-oxo-guanine. *Proceedings of the National Academy of Sciences*, *95*(1), 288–293. <https://doi.org/10.1073/pnas.95.1.288>
- Hu, C. W., Chao, M. R., & Sie, C. H. (2010). Urinary analysis of 8-oxo-7,8-dihydroguanine and 8-oxo-7,8-dihydro-2'-deoxyguanosine by isotope-dilution LC-MS/MS with automated solid-phase extraction: Study of 8-oxo-7,8-dihydroguanine stability. *Free Radical Biology and Medicine*, *48*(1), 89–97. <https://doi.org/10.1016/j.freeradbiomed.2009.10.029>
- Hudson, E. K., Hogue, B. A., Souza-Pinto, N. C., Croteau, D. L., Anson, R. M., Bohr, V. A., & Hansford, R. G. (1998). Age-associated change in mitochondrial DNA damage. *Free Radical Research*, *29*(6), 573–579. <https://doi.org/10.1080/10715769800300611>
- Hurley, M. J., Brandon, B., Gentleman, S. M., & Dexter, D. T. (2013). Parkinson's disease is associated with altered expression of CaV1 channels and calcium-binding proteins. *Brain*, *136*(Pt 7), 2077–2097. <https://doi.org/10.1093/brain/awt134>
- Hurley, M. J., Gentleman, S. M., & Dexter, D. T. (2015). Calcium CaV1 channel subtype mRNA expression in Parkinson's disease examined by in situ hybridization. *Journal of Molecular Neuroscience*, *55*(4), 715–724. <https://doi.org/10.1007/s12031-014-0410-8>
- Isobe, C., Abe, T., & Terayama, Y. (2010). Levels of reduced and oxidized coenzyme Q-10 and 8-hydroxy-2'-deoxyguanosine in the cerebrospinal fluid of patients with living Parkinson's disease demonstrate that mitochondrial oxidative damage and/or oxidative DNA damage contributes to the neurodegenerative process. *Neuroscience Letters*, *469*(1), 159–163. <https://doi.org/10.1016/j.neulet.2009.11.065>
- Ivashkevich, A., Redon, C. E., Nakamura, A. J., Martin, R. F., & Martin, O. A. (2012). Use of the gamma-H2AX assay to monitor DNA damage and repair in translational cancer research. *Cancer Letters*, *327*(1-2), 123–133. <https://doi.org/10.1016/j.canlet.2011.12.025>
- Jackson, S. P., & Bartek, J. (2009). The DNA-damage response in human biology and disease. *Nature*, *461*(7267), 1071–1078. <https://doi.org/10.1038/nature08467>
- Kang, S., Cooper, G., Dunne, S. F., Dusel, B., Luan, C. H., Surmeier, D. J., & Silverman, R. B. (2012). Cav1.3-selective L-type calcium channel antagonists as potential new therapeutics for Parkinson's disease. *Nature Communications*, *3*, 1146. <https://doi.org/10.1038/ncomms2149>
- Karahalil, B., Miser Salihoglu, E., Elkama, A., Orhan, G., Saygin, E., & Yardim Akaydin, S. (2022). Individual susceptibility has a major impact on strong association between oxidative stress, defence systems and Parkinson's disease. *Basic & Clinical Pharmacology & Toxicology*, *130*(1), 158–170. <https://doi.org/10.1111/bcpt.13659>
- Karreman, M., & Moghaddam, B. (1996). Effect of a pharmacological stressor on glutamate efflux in the prefrontal cortex. *Brain Research*, *716*(1-2), 180–182. [https://doi.org/10.1016/0006-8993\(96\)00015-7](https://doi.org/10.1016/0006-8993(96)00015-7)
- Kastan, M. B., & Bartek, J. (2004). Cell-cycle checkpoints and cancer. *Nature*, *432*(7015), 316–323. <https://doi.org/10.1038/nature03097>

- Kim, K. H., Yoo, H. Y., Joo, K. M., et al. (2011). Time-course analysis of DNA damage response-related genes after in vitro radiation in H460 and H1229 lung cancer cell lines. *Experimental and Molecular Medicine*, 43(7), 419–426. <https://doi.org/10.3858/emm.2011.43.7.046>
- Kinner, A., Wu, W., Staudt, C., & Iliakis, G. (2008). Gamma-H2AX in recognition and signaling of DNA double-strand breaks in the context of chromatin. *Nucleic Acids Research*, 36(17), 5678–5694. <https://doi.org/10.1093/nar/gkn550>
- Kiptoo, M. K., Mpoke, S. S., & Ng'ang'a, Z. W. (2004). New indirect immunofluorescence assay as a confirmatory test for human immunodeficiency virus type 1. *East African Medical Journal*, 81(5), 222–225. <https://doi.org/10.4314/eamj.v81i5.9163>
- Kryston, T. B., Georgiev, A. B., Pissis, P., & Georgakilas, A. G. (2011). Role of oxidative stress and DNA damage in human carcinogenesis. *Mutation Research/Fundamental and Molecular Mechanisms of Mutagenesis*, 711(1-2), 193–201. <https://doi.org/10.1016/j.mrfmmm.2010.12.016>
- Lang, Y., Gong, D., & Fan, Y. (2015). Calcium channel blocker use and risk of Parkinson's disease: A meta-analysis. *Pharmacoeconomics and Drug Safety*, 24(6), 559–566. <https://doi.org/10.1002/pds.3781>
- Livak, K. J., & Schmittgen, T. D. (2001). Analysis of relative gene expression data using real-time quantitative PCR and the 2(-Delta Delta C(T)) method. *Methods (San Diego, Calif.)*, 25(4), 402–408. <https://doi.org/10.1006/meth.2001.1262>
- Lotharius, J., & Brundin, P. (2002). Pathogenesis of Parkinson's disease: Dopamine, vesicles and alpha-synuclein. *Nature Reviews Neuroscience*, 3(12), 932–942. <https://doi.org/10.1038/nrn983>
- Massudi, H., Grant, R., Braidy, N., Guest, J., Farnsworth, B., & Guillemin, G. J. (2012). Age-associated changes in oxidative stress and NAD+ metabolism in human tissue. *PLoS one*, 7(7), e42357. <https://doi.org/10.1371/journal.pone.0042357>
- McMillan, T. J., Leatherman, E., Ridley, A., Shorrocks, J., Tobi, S. E., & Whiteside, J. R. (2008). Cellular effects of long wavelength UV light (UVA) in mammalian cells. *Journal of Pharmacy and Pharmacology*, 60(8), 969–976. <https://doi.org/10.1211/jpp.60.8.0004>
- Mecocci, P., Fano, G., Fulle, S., et al. (1999). Age-dependent increases in oxidative damage to DNA, lipids, and proteins in human skeletal muscle. *Free Radical Biology and Medicine*, 26(3-4), 303–308. [https://doi.org/10.1016/S0891-5849\(98\)00208-1](https://doi.org/10.1016/S0891-5849(98)00208-1)
- Meiser, J., Weindl, D., & Hiller, K. (2013). Complexity of dopamine metabolism. *Cell Communication and Signaling*, 11(1), 34. <https://doi.org/10.1186/1478-811X-11-34>
- Merlo, D., Mollinari, C., Racaniello, M., Garaci, E., & Cardinale, A. (2016). DNA Double strand breaks: A common theme in neurodegenerative diseases. *Current Alzheimer Research*, 13(11), 1208–1218. <https://doi.org/10.2174/1567205013666160401114915>
- Migliore, L., Petrozzi, L., Lucetti, C., et al. (2002). Oxidative damage and cytogenetic analysis in leukocytes of Parkinson's disease patients. *Neurology*, 58(12), 1809–1815. <https://doi.org/10.1212/WNL.58.12.1809>
- Migliore, L., Scarpato, R., Coppede, F., Petrozzi, L., Bonuccelli, U., & Rodilla, V. (2001). Chromosome and oxidative damage biomarkers in lymphocytes of Parkinson's disease patients. *International Journal of Hygiene and Environmental Health*, 204(1), 61–66. <https://doi.org/10.1078/1438-4639-00074>
- Milanese, C., Cerri, S., Ulusoy, A., et al. (2018). Activation of the DNA damage response in vivo in synucleinopathy models of Parkinson's disease. *Cell Death & Disease*, 9(8), 818. <https://doi.org/10.1038/s41419-018-0848-7>
- Miyazaki, I., & Asanuma, M. (2008). Dopaminergic neuron-specific oxidative stress caused by dopamine itself. *Acta Medica Okayama*, 62(3), 141–150.
- Mooslehner, K. A., Chan, P. M., Xu, W., Liu, L., Smadja, C., Humby, T., Allen, N. D., Wilkinson, L. S., & Emson, P. C. (2001). Mice with very low expression of the vesicular monoamine transporter 2 gene survive into adulthood: Potential mouse model for parkinsonism. *Molecular and Cellular Biology*, 21(16), 5321–5331. <https://doi.org/10.1128/MCB.21.16.5321-5331.2001>
- Mullaart, E., Boerrieger, M. E., Ravid, R., Swaab, D. F., & Vijg, J. (1990). Increased levels of DNA breaks in cerebral cortex of Alzheimer's disease patients. *Neurobiology of Aging*, 11(3), 169–173. [https://doi.org/10.1016/0197-4580\(90\)90542-8](https://doi.org/10.1016/0197-4580(90)90542-8)
- Olson, P. A., Tkatch, T., Hernandez-Lopez, S., Ulrich, S., Ilijic, E., Mugnaini, E., Zhang, H., Bezprozvanny, I., & Surmeier, D. J. (2005). G-protein-coupled receptor modulation of striatal CaV1.3 L-type Ca2+ channels is dependent on a shank-binding domain. *Journal of Neuroscience*, 25(5), 1050–1062. <https://doi.org/10.1523/JNEUROSCI.3327-04.2005>
- O'Neill, P., & Wardman, P. (2009). Radiation chemistry comes before radiation biology. *International Journal of Radiation Biology*, 85(1), 9–25. <https://doi.org/10.1080/09553000802640401>
- Orrenius, S., Zhivotovsky, B., & Nicotera, P. (2003). Regulation of cell death: The calcium-apoptosis link. *Nature Reviews Molecular Cell Biology*, 4(7), 552–565. <https://doi.org/10.1038/nrm1150>
- Rappold, I., Iwabuchi, K., Date, T., & Chen, J. (2001). Tumor suppressor p53 binding protein 1 (53BP1) is involved in DNA damage-signaling pathways. *Journal of Cell Biology*, 153(3), 613–620. <https://doi.org/10.1083/jcb.153.3.613>
- Sanchez-Padilla, J., Guzman, J. N., Ilijic, E., et al. (2014). Mitochondrial oxidant stress in locus coeruleus is regulated by activity and nitric oxide synthase. *Nature Neuroscience*, 17(6), 832–840. <https://doi.org/10.1038/nn.3717>
- Sato, S., Mizuno, Y., & Hattori, N. (2005). Urinary 8-hydroxydeoxyguanosine levels as a biomarker for progression of Parkinson disease. *Neurology*, 64(6), 1081–1083. <https://doi.org/10.1212/01.WNL.0000154597.24838.6B>
- Schultz, L. B., Chehab, N. H., Malikzay, A., & Halazonetis, T. D. (2000). P53 binding protein 1 (53BP1) is an early participant in the cellular response to DNA double-strand breaks. *Journal of Cell Biology*, 151(7), 1381–1390. <https://doi.org/10.1083/jcb.151.7.1381>
- Shao, C., Xiong, S., Li, G. M., Gu, L., Mao, G., Markesbery, W. R., & Lovell, M. A. (2008). Altered 8-oxoguanine glycosylase in mild cognitive impairment and late-stage Alzheimer's disease brain. *Free Radical Biology and Medicine*, 45(6), 813–819. <https://doi.org/10.1016/j.freeradbiomed.2008.06.003>
- Shigenaga, M. K., Gimeno, C. J., & Ames, B. N. (1989). Urinary 8-hydroxy-2'-deoxyguanosine as a biological marker of in vivo oxidative DNA damage. *Proceedings of the National Academy of Sciences*, 86(24), 9697–9701. <https://doi.org/10.1073/pnas.86.24.9697>
- Shimura-Miura, H., Hattori, N., Kang, D., Miyako, K., Nakabeppu, Y., & Mizuno, Y. (1999). Increased 8-oxo-dGTPase in the mitochondria of substantia nigral neurons in Parkinson's disease.

- Annals of Neurology*, 46(6), 920–924. [https://doi.org/10.1002/1531-8249\(199912\)46:6<920::AID-ANA17>3.0.CO;2-R](https://doi.org/10.1002/1531-8249(199912)46:6<920::AID-ANA17>3.0.CO;2-R)
- Souza-Pinto, N. C., Croteau, D. L., Hudson, E. K., Hansford, R. G., & Bohr, V. A. (1999). Age-associated increase in 8-oxo-deoxyguanosine glycosylase/AP lyase activity in rat mitochondria. *Nucleic Acids Research*, 27(8), 1935–1942. <https://doi.org/10.1093/nar/27.8.1935>
- Surguchov, A. (2022). Biomarkers in Parkinson's disease. In P. V. Peplow, B. Martinez, & T. A. Gennarelli (Eds.), *Neurodegenerative diseases biomarkers. Neuromethods* (pp. 155–180). Humana.
- Taylor, T. N., Alter, S. P., Wang, M., Goldstein, D. S., & Miller, G. W. (2014). Reduced vesicular storage of catecholamines causes progressive degeneration in the locus coeruleus. *Neuropharmacology*, 76 Pt A, 97–105. <https://doi.org/10.1016/j.neuropharm.2013.08.033>
- Taylor, T. N., Caudle, W. M., & Miller, G. W. (2011). VMAT2-Deficient Mice display nigral and extranigral pathology and motor and nonmotor symptoms of Parkinson's disease. *Parkinson's Disease*, 2011, 1–9. <https://doi.org/10.4061/2011/124165>
- Taylor, T. N., Caudle, W. M., Shepherd, K. R., Noorian, A., Jackson, C. R., Iuvone, P. M., Weinshenker, D., Greene, J. G., & Miller, G. W. (2009). Nonmotor symptoms of Parkinson's disease revealed in an animal model with reduced monoamine storage capacity. *Journal of Neuroscience*, 29(25), 8103–8113. <https://doi.org/10.1523/JNEUROSCI.1495-09.2009>
- Temple, M. D., Perrone, G. G., & Dawes, I. W. (2005). Complex cellular responses to reactive oxygen species. *Trends in Cell Biology*, 15(6), 319–326. <https://doi.org/10.1016/j.tcb.2005.04.003>
- Uttara, B., Singh, A. V., Zamboni, P., & Mahajan, R. T. (2009). Oxidative stress and neurodegenerative diseases: A review of upstream and downstream antioxidant therapeutic options. *Current Neuropharmacology*, 7(1), 65–74. <https://doi.org/10.2174/157015909787602823>
- Valavanidis, A., Vlachogianni, T., & Fiotakis, C. (2009). 8-hydroxy-2'-deoxyguanosine (8-OHdG): A critical biomarker of oxidative stress and carcinogenesis. *Journal of Environmental Science and Health. Part C, Environmental Carcinogenesis & Ecotoxicology Reviews*, 27(2), 120–139.
- Wang, B., Matsuoka, S., Carpenter, P. B., & Elledge, S. J. (2002). 53BP1, A mediator of the DNA damage checkpoint. *Science (New York, N.Y.)*, 298(5597), 1435–1438. <https://doi.org/10.1126/science.1076182>
- Wang, D., Yu, T., Liu, Y., Yan, J., Guo, Y., Jing, Y., Yang, X., Song, Y., & Tian, Y. (2016). DNA Damage preceding dopamine neuron degeneration in A53T human alpha-synuclein transgenic mice. *Biochemical and Biophysical Research Communications*, 481(1-2), 104–110. <https://doi.org/10.1016/j.bbrc.2016.11.008>
- Wang, J., Xiong, S., Xie, C., Markesbery, W. R., & Lovell, M. A. (2005). Increased oxidative damage in nuclear and mitochondrial DNA in Alzheimer's disease. *Journal of Neurochemistry*, 93(4), 953–962. <https://doi.org/10.1111/j.1471-4159.2005.03053.x>
- Ward, J. F. (1988). DNA Damage produced by ionizing radiation in mammalian cells: Identities, mechanisms of formation, and reparability. *Progress in Nucleic Acid Research and Molecular Biology*, 35(1), 95–125. [https://doi.org/10.1016/S0079-6603\(08\)60611-X](https://doi.org/10.1016/S0079-6603(08)60611-X)
- Weissman, L., Jo, D. G., Sorensen, M. M., de Souza-Pinto, N. C., Markesbery, W. R., Mattson, M. P., & Bohr, V. A. (2007). Defective DNA base excision repair in brain from individuals with Alzheimer's disease and amnesic mild cognitive impairment. *Nucleic Acids Research*, 35(16), 5545–5555. <https://doi.org/10.1093/nar/gkm605>
- Williams, J. T., North, R. A., Shefner, S. A., Nishi, S., & Egan, T. M. (1984). Membrane properties of rat locus coeruleus neurons. *Neuroscience*, 13(1), 137–156. [https://doi.org/10.1016/0306-4522\(84\)90265-3](https://doi.org/10.1016/0306-4522(84)90265-3)
- Zhang, J., Perry, G., Smith, M. A., Robertson, D., Olson, S. J., Graham, D. G., & Montine, T. J. (1999). Parkinson's disease is associated with oxidative damage to cytoplasmic DNA and RNA in substantia nigra neurons. *The American Journal of Pathology*, 154(5), 1423–1429. [https://doi.org/10.1016/S0002-9440\(10\)65396-5](https://doi.org/10.1016/S0002-9440(10)65396-5)
- Zhou, B. B., & Elledge, S. J. (2000). The DNA damage response: Putting checkpoints in perspective. *Nature*, 408(6811), 433–439. <https://doi.org/10.1038/35044005>
- Zhu, M. Y., Raza, M. U., Zhan, Y., & Fan, Y. (2019). Norepinephrine upregulates the expression of tyrosine hydroxylase and protects dopaminergic neurons against 6-hydrodopamine toxicity. *Neurochemistry International*, 131, 104549. <https://doi.org/10.1016/j.neuint.2019.104549>
- Zhu, M. Y., Wang, W. P., & Bissette, G. (2006). Neuroprotective effects of agmatine against cell damage caused by glucocorticoids in cultured rat hippocampal neurons. *Neuroscience*, 141(4), 2019–2027. <https://doi.org/10.1016/j.neuroscience.2006.05.011>
- Zlatkovic, J., Todorovic, N., Boskovic, M., Pajovic, S. B., Demajo, M., & Filipovic, D. (2014). Different susceptibility of prefrontal cortex and hippocampus to oxidative stress following chronic social isolation stress. *Molecular and Cellular Biochemistry*, 393(1-2), 43–57. <https://doi.org/10.1007/s11010-014-2045-z>